Department of Chemical and Metallurgical Engineering

Concentration of Aqueous Solutions by Freeze Crystallization in Biorefinery Applications

Nahla Osmanbegovic

Aalto University

DOCTORAL THESES

Aalto University publication series
DOCTORAL THESES 138/2023

Concentration of Aqueous Solutions by Freeze Crystallization in Biorefinery Applications

Nahla Osmanbegovic

A doctoral thesis completed for the degree of Doctor of Science (Technology) to be defended, with the permission of the Aalto University School of Chemical Engineering, at a public examination held at the lecture hall Ke2 of the school on 15th of September 2023 at 13:00.

Aalto University
School of Chemical Engineering
Department of Chemical and Metallurgical Engineering
Chemical Engineering in Aqueous Systems

Supervising professor
Professor Marjatta Louhi-Kultanen, Aalto University, Finland

Thesis advisor
Doctor Han Bing, Aalto University, Finland

Preliminary examiners
Professor Alison Lewis, University of Cape Town, South Africa
Professor Burak Eral, Delft University of Technology, The Netherlands

Opponent
Professor Kerstin Forsberg, KTH Royal Institute of Technology, Sweden

Aalto University publication series
DOCTORAL THESES 138/2023

ISBN 978-952-64-1412-6 (printed)
ISBN 978-952-64-1413-3 (pdf)
ISSN 1799-4934 (printed)
ISSN 1799-4942 (pdf)
http://urn.fi/URN:ISBN:978-952-64-1413-3

Unigrafia Oy
Helsinki 2023

Finland

NORDIC SWAN ECOLABEL
Printed matter
4041-0619

Author
Nahla Osmanbegovic

Name of the doctoral thesis
Concentration of Aqueous Solutions by Freeze Crystallization in Biorefinery Applications

Publisher School of Chemical Engineering

Unit Department of Chemical and Metallurgical Engineering

Series Aalto University publication series DOCTORAL THESES 138/2023

Field of research Chemical Engineering in Aqueous Systems

Manuscript submitted 10 May 2023 **Date of the defence** 15 September 2023

Permission for public defence granted (date) 18 August 2023 **Language** English

☐ **Monograph** ☒ **Article thesis** ☐ **Essay thesis**

Abstract

Freeze crystallization (FC) is a melt crystallization method, defined as water removal based on ice formation and its separation from aqueous solutions at or slightly below the freezing point of the solution. In this work,freeze crystallization (suspension freeze (SFC) and layer freeze crystallization (LFC)) was applied as a concentration method for different aqueous organic solutions obtained in the emerging fields of biorefinery applications, where a concentration step is typically required in downstream processing.The studied aqueous solutions were 1,5-diazabicyclo[4.3.0]non-5-eniumacetate ([DBNH][OAc]) ionic liquid solution, aqueous pyrolysis oil (PO) extract, acetone-1-butanol-ethanol (ABE) fermentation broths, and synthetic sucrose and ABE solutions. SFC and LFC were applied to concentrate solutions with freezing points in the range from -0.56°C to -7.51°C.The ice nucleation and growth kinetics were influenced to varying degrees by the solution ideality, undercooling, and initial water concentration in feed solution. The ice yields of various solutions obtained by SFC for undercooling degrees in the range of 0.39-1.87 °C were as follows: 19.8-35.6 % for [DBNH][OAc] solutions (60 min freezing),11.6–68% for PO extract (60 min freezing), and 54.6-86.7% for ABE fermentation broths (80 min freezing).The concentration of impurities in washed ice samples was below the detection limit hence the distribution coefficients were effectively zero for PO extract and ABE solutions, and up to 0.26 for [DBNH][OAc] solutions. Hence, SFC was found to be a very efficient concentration method that removes water in the form of very pure ice with high yields.The ice yields for LFC were lower than for SFC because of the smaller cooling area. Thus, the obtained ice yields for 60 min of freezing at an undercooling range of 0.83-2.28 °C were:1.3-5.8% for aqueous sucrose solution and 3.6-7.15% for [DBNH][OAc] solutions with 60 min of freezing. The heat transfer during cooling of aqueous solutions (10 wt.%, 23 wt.% and 30 wt.% sucrose) prior to ice layer formation was investigated by CFD simulations. The solution properties affected the cooling in such a way that the less concentrated the solution was, the faster the undercooling temperature (supersaturation) was reached, and consequently the convective heat transfer coefficient values were higher. SFC enabled the separation of 1-butanol from synthetic ABE solutions, with average cumulative yields of separated 1-butanol were in range 9.6-59.5% and with purities in the range of 84.8-94.9%. Cooling crystallization from solutions was applied as a levoglucosan recovery method from PO extract. The average recovery levoglucosan rate achieved was 24%. In conclusion, FC is an efficient method for concentrating various biorefinery related solutions. Moreover, it enables separation of sparingly miscible 1-butanol from ABE solutions. Furthermore, cooling crystallization from solutions can be considered as a recovery method for valuable biochemicals, such as levoglucosan, from aqueous PO extracts.

Keywords freeze crystallization, concentration, recovery, biorefinery

ISBN (printed) 978-952-64-1412-6 **ISBN (pdf)** 978-952-64-1413-3

ISSN (printed) 1799-4934 **ISSN (pdf)** 1799-4942

Location of publisher Helsinki **Location of printing** Helsinki **Year** 2023

Pages 98 **urn** http://urn.fi/URN:ISBN:978-952-64-1413-3

Acknowledgements

"From many stages travelers must ascend
Until one day they reach the journey's end.
Iron's not red, in fire though red it turns
Due to the heat of flames in which it burns…
…Whoever tried this journey on his own
The guides still helped – he didn't walk alone."
Rumi

All praise belongs to the Almighty, who inspires me to embark on the journey of seeking knowledge. The valuable lesson I have learned during my PhD studies is that the key for every personal success are people who offer us an intellectual, moral, and emotional guidance and support.

I would like to express my gratitude to my supervisor Marjatta Louhi-Kultanen who has guided me from the very beginning of my doctoral studies, helped me through the ups and downs of my research and taught me that there is always a way to achieve results if I embrace different perspectives.

I would also like to thank my thesis advisor Han Bing for helping me to smoothly transition from theoretical to experimental research and for giving me valuable feedbacks on my research progress.

I am sincerely grateful to Prof. Dr. Heike Lorenz that hosted me at Max-Planck Institute Magdeburg and collaborated with us on our first publication. I am thankful to my co-authors, Ville Alopaeus, Ville Vuorinen, Jukka Konttinen, Sandip Bankar, Lina Yuan, Vijaya Chandgude and Anubhuti Bhatnagar for insightful comments and fruitful collaborations.

Special thanks go to Petri Uusi-Kyyny and Juha-Pekka Pokki that were always eager to navigate me through laboratories and various equipment, and to Seppo Jääskeläinen who designed and built the melt crystallization platform and assisted me with all necessary adjustments needed for different projects.

I am thankful to my current and former colleagues, Ila Mitra, Zhang Jianxin, Anna Zaykovskaya, Arshe Said and Mani Rajaboopathi for creating a pleasant and encouraging working environment.

During my PhD, I have been lucky to have incredible friends by my side. Adna, Sushilika, Bahareh, Zahra, Elham, Sudatta, Vijaya and Anubhuti, thank you for inspirational conversations and many memorable memories.

This journey would not be possible without my biggest emotional support - my dear parents, Fadila and Nezir, and my dearest sister Nedžla. Thank you for believing in me, encouraging me and never letting me give up on my dreams.

Helsinki, August 2023
Nahla Osmanbegović

Contents

List of Abbreviations and Symbols 2
List of Publications 4
Author's Contribution 5
1. Introduction 6
1.1 Background 6
1.2 Freeze crystallization 8
1.3 Research objectives 9
2. Experimental Methodology 12
2.1 Aqueous solutions studied 12
2.2 Suspension freeze crystallization 13
2.3 Layer freeze crystallization 14
2.4 Analytical methods 16
3. Thermodynamics of freeze crystallization 17
3.1 Freezing points of aqueous solutions 17
3.2 Solution ideality 20
4. Kinetics of freeze crystallization 21
4.1 Ice nucleation rate and overall crystal growth rate 21
4.2 Separation efficiency 24
4.3 Ice morphology 28
5. CFD study on heat transfer 30
6. 1 – butanol separation from synthetic ABE solutions 35
7. Levoglucosan recovery from pyrolysis oil 38
8. Summary 41
References 44

List of Abbreviations and Symbols

ABE	acetone-1-butanol-ethanol
ABEW	acetone-1-butanol-ethanol-water
CFD	computational fluid dynamics
[DBNH][OAc]	1,5-diazabicyclo[4.3.0]non-5-enium acetate
GC	gas chromatography
HPLC	high-performance liquid chromatography
LFC	layer freeze crystallization
[mTBDH][OAc]	7-methyl-1,5,7-triazabicyclo[4.4.0] dec-5-enium acetate
PO	pyrolysis oil
SEM	scanning electron microscopy
SFC	suspension freeze crystallization
TOC	total organic carbon
XRD	x-ray diffraction

β	nucleation rate of a single ice crystal
γ	activity coefficient
μ^{o}_{2}	second moment of ice seed crystal distribution
χ	mol fraction
ΔT	undercooling degree
$C_{solute,ice}$	solute concentration in ice
$C_{solute,feed}$	solute concentration in feed solution
$(dT/dt)_{max}$	maximum slope of the temperature response curve
h	convective heat transfer coefficient
K	distribution coefficient

$m_{ice,pure}$	mass of a pure ice
$m_{water,feed}$	mass of water in feed solution
q_i	heat flux
$R_{G,ice}$	overall ice growth rate
T	solution temperature
T_i	temperature of a cooling surface
t	time
U_i	overall heat transfer coefficient
Y	ice yield
z	vertical axis

List of Publications

This doctoral dissertation consists of a summary and of the following publications which are referred to in the text by their numerals

1. Osmanbegovic, Nahla; Yuan, Lina; Heike, Lorenz; Louhi-Kultanen, Marjatta. 2020. Freeze Concentration of Aqueous [DBNH][OAc] Ionic Liquid Solution. MDPI. Crystals, vol. 10, no. 3, p. 147. DOI 10.3390/cryst10030147.

2. Osmanbegovic, Nahla; Alopaeus, Ville; Han, Bing; Vuorinen, Ville; Louhi-Kultanen, Marjatta. 2022. Experimental and CFD Study on Influence of Viscosity on Layer Melt Crystallization. Elsevier. Separation and Purification Technology, vol. 284, p. 120170. DOI 10.1016/j.seppur.2021.120170.

3. Osmanbegovic, Nahla; Chandgude, Vijaya; Bankar, Sandip; Louhi-Kultanen, Marjatta. 2023. 1-Butanol Separation from Aqueous Acetone-Butanol-Ethanol (ABE) Solutions by Freeze Concentration. ACS. Crystal Growth & Design, vol. 23, no. 6, p. 4147-4153. DOI 10.1021/acs.cgd.2c01546.

4. Osmanbegovic, Nahla; Bhatnagar, Anubhuti; Konttinen, Jukka; Louhi-Kultanen, Marjatta. 2023. Freeze concentration of aqueous pyrolysis oil extract and levoglucosan recovery by cooling crystallization. Elsevier. Powder Technology, vol. 427, p. 118700. DOI 10.1016/j.powtec.2023.118700

Author's Contribution

Paper 1: Freeze Concentration of Aqueous [DBNH][OAc] Ionic Liquid Solution

NO developed the experimental procedure and performed layer and suspension freeze crystallization experiments under the supervision of MLK. NO wrote and edited the manuscript based on revisions made by MLK. LY performed the DSC analysis and contributed to manuscript writing related to DSC methods and results under the supervision of HL.

Paper 2: Experimental and CFD Study on Influence of Viscosity on Layer Melt Crystallization

NO conducted the layer freeze crystallization experiments, developed the CFD model, and performed the simulations. NO wrote and edited the manuscript based on the comments and revisions made by MLK, VA and VV. The experimental part of the study was supervised by MLK and HB. The CFD study was supervised by VA and VV.

Paper 3: 1-Butanol Separation from Aqueous Acetone-Butanol-Ethanol (ABE) Solutions by Freeze Concentration

NO developed the experimental procedure and performed the experiments based on suspension freeze crystallization and liquid-liquid extraction for 1-butanol separation. NO characterized the samples (ice, water-enriched phase, 1-butanol phase) using the GC and TOC analytical methods. NO wrote and edited the manuscript based on comments and revision made by MLK. MLK supervised the freeze crystallization study. VC produced the ABE fermentation broths and wrote a section in the manuscript related to the production of ABE fermentation broths under the supervision of SB.

Paper 4: Freeze Concentration of Aqueous Pyrolysis Oil Extract and Levoglucosan Recovery by Cooling Crystallization

NO conducted the suspension freeze crystallization and cooling crystallization experiments, performed analyses on the ice and levoglucosan samples based on TOC, XRD, SEM, DSC, PSD methods under the supervision of MLK. AB performed pyrolysis and the composition analysis of the pyrolysis oil and mother liquors produced based on HPLC and GC under the supervision of JK. NO and AB wrote the manuscript and revised it based on comments by MLK and JK.

1. Introduction

1.1 Background

The growing human population is leading to rising food and energy demands with increasing challenges to properly manage waste generation. Meeting these demands is complicated by political instability, very often more than by the lack of natural resources. Another challenge is assuring society's transition toward the implementation of sustainability and circular economy principles from industrial production, through transportation to goods consumption, to reduce the severe negative effects of global warming. Industry has been the key for economic development, but it must be revolutionized with the implementation of novel technologies that will be less energy consuming and with emissions reduced to a minimum (1). The International Energy Agency (IEA) reported that global energy consumption related to industrial production in 2021 was 38% (2). The chemical industry is one of the main energy consumers, especially for thermal separation processes based on evaporation, such as distillation, that account for around 40% of the total global energy consumed in the chemical industry (3). However, separation technologies are key units of downstream processing that encompasses different methods for the separation of chemicals, the purification of the final product, product recovery, and recycling (4). Therefore, the development and application of novel industrial separation methods has become one of the important objectives in various sectors of industry from metal, material, and forest product processing to food, the pharmaceutical industry, and wastewater treatment (5, 6).

The main objective of this thesis was to investigate freeze crystallization as a concentration method for multi-compound organic mixtures produced in various biorefinery applications.

The importance of the biorefinery has been growing as the implementation of sustainability and circular economy principles is becoming mandatory. Biomass is converted into biofuel, biochemicals, and bioproducts via biorefinery concepts, such as pyrolysis and fermentation through thermochemical and biochemical conversions, respectively. These are potential processes that can replace the conventional process in petrochemical refineries that uses fossil resources (7-10).

Pyrolysis oil obtained by slow or fast pyrolysis is a complex mixture of various organic compounds, namely organic acids, ketones, and phenols. Hence, it can be considered as a perfect source for the extraction of platform biochemicals, such as levoglucosan and vanillin, that can find further application in biopolymer synthesis, and the pharmaceutical and food industry, respectively. The current research also focuses on different upgrading methods to convert pyrolysis oil into a potentially stable fuel (11-13).

Fermentation of cellulosic material enabled by using Clostridium species is a type of biochemical conversion that results in the production of acetone-1-butanol-ethanol (ABE)

fermentation broth. ABE fermentation is important regarding the production of biobutanol, which can be considered as a potential replacement for fossil fuels such as diesel. The enhancement of biobutanol production from various cellulosic resources with ABE fermentation has been studied previously (14-17).

Moreover, a novel biorefinery concept named Ioncell®, a process in which cellulose dissolution occurs with the application of ionic liquid solvents, enables the production of a new type of sustainable fibers, so-called "man-made fibers". The process has the potential to revolutionize the textile industry with benefits such as the replacement not only of synthetic fibers, but also natural fibers, namely cotton, which would significantly reduce the water consumption necessary for cotton cultivation and increase the available cultivated area for agricultural purposes and food production in countries with a rapidly growing population (18-21).

Downstream processing in a biorefinery, especially the separation and purification methods of target biochemicals from multi-component aqueous mixtures produced by pyrolysis and fermentation, is a key area that needs to be investigated and properly developed for wider industrial applications of the above-mentioned biorefinery concepts (22).

Furthermore, application of a suitable recycling technique for the ionic liquid solvents used in the Lyocell process is needed, because they are relatively expensive and, even though considered "green solvents," can still have toxic and harmful effects on the environment (23, 24). Hence, ionic liquid recycling can significantly contribute to the commercialization and competitiveness of Ioncell® as a green, sustainable, and economically feasible technology.

Extensive research has been conducted on various separation methods that can potentially be applicable for the recovery of ionic liquids from aqueous solutions, biobutanol recovery from ABE fermentation broth, and separation of biochemicals from pyrolysis oil (25-32).

Adsorption has been studied as a method for the recovery of ionic liquids in a low concentration range from aqueous solutions (33-36), for the separation of sugars and phenolics from pyrolysis oil (37), and for biobutanol recovery from ABE fermentation broth (38).

Various distillation-based methods, such as molecular distillation (39-41) and vacuum distillation (42, 43), have been reported as separation methods for ionic liquids and pyrolysis oil, as has vapor compression distillation (44) for solvent recovery from ABE solutions.

Membrane-based methods, such as membrane distillation (45-48) and pervaporation (49-52), have been studied for ionic liquid and butanol recovery. Nanofiltration and electrodialysis (53, 54) have been reported as separation methods for ionic liquids from aqueous solutions and nanofiltration combined with reverse osmosis has been used as a method for acid recovery from aqueous phase of pyrolysis oil (55).

Liquid-liquid extraction enabled by various solvents has been reported for the recovery of ionic liquids, products from pyrolysis oil, and solvents from ABE solutions (56-58).

Gas stripping integrated with ABE fermentation has also been investigated as a promising method for ABE solvent recovery (59-61).

The disadvantages of the above-mentioned processes are discussed below. Adsorption can be suitable for the recovery of organic compounds that are present in a low concentration range in aqueous solutions depending on the adsorbent surface chemistry (31). Distillation is not only an energy-intensive method but is also unsuitable for thermally unstable organic compounds like ionic liquids and systems that form an azeotrope like butanol in aqueous solutions (26, 31, 32). Membrane separation requires cleaning after a few operating cycles and

organics cause membrane fouling (31, 62). Extraction process efficiency depends on finding suitable, relatively cheap, and non-toxic solvents with good selectivity (31, 33, 58). Moreover, it is necessary to regenerate the organic solvents used in liquid-liquid extraction.
Freeze crystallization has not been studied as a method for butanol recovery, even though it is mentioned as a potential method in the literature (63). However, a theoretical study on the energy consumption of an ionic liquid recycling process based on freeze crystallization and evaporation, and an experimental study on freeze crystallization as a potential treatment for wastewater produced in a pyrolysis plant have been reported in earlier studies (64, 65).

1.2 Freeze crystallization

Freeze crystallization (FC) is a type of melt crystallization where water is removed in the form of ice crystals from an aqueous solution at its freezing temperature. The main driving force for freeze crystallization to occur is undercooling, caused by the temperature difference between the surface of the growing ice crystals and the surrounding aqueous solution. Water removal from aqueous systems in the form of ice uses 14% of the energy needed for water removal in the form of vapor in evaporation methods, as a direct result of the difference between the latent heats of freezing and vaporization. In the case of dilute aqueous solutions, when the solution is cooled below the freezing point according to the liquidus line of solid-liquid equilibria (SLE), only water forms a solid as ice. Thus, no pretreatment is needed prior to FC, which makes FC a robust concentration method for multi-component solutions.
Two methods of freeze crystallization can be distinguished: layer freeze and suspension freeze, based on how ice crystals form and grow in aqueous solutions.
Layer freeze crystallization is a method where the formation and growth of ice crystals from the aqueous solution occur in the form of a layer on the undercooled surface of the crystallizer. Layer freeze crystallization can be performed in static (stagnant) or dynamic falling film mode. In the case of static layer freeze crystallization, the ice layer is formed from stagnant aqueous solutions on the undercooled surfaces of heat exchangers (66). Dynamic layer freeze crystallization is characterized by the circulation of aqueous feed solution over crystallizer heat exchanger tubes, usually in the form of a falling film (67, 68).
Suspension freeze crystallization refers to the formation and growth of dispersed ice crystals inside a stirred aqueous solution. The stirrer acts as a scraper that prevents ice incrustation on the inner walls of the crystallizer.
The above-mentioned methods have their respective advantages and disadvantages (69). A layer freeze crystallizer has a simple configuration as there is no need for moving equipment and it is suitable for highly viscous solutions. However, heat transfer is limited with a growing ice layer that acts as an insulator between the solution and undercooled surface, which results in a limited ice yield.
Crystallizers with rotating scrapers used for suspension freeze crystallization have a more complex design and need better maintenance than the crystallizer for layer freeze crystallization. However, the ice yields obtained are higher than in the case of layer freeze crystallization due to the higher cooling surface area. Ice purity is further increased by a washing step performed in a washing column (66, 70).
Freeze crystallization methods are commonly implemented for the concentration of various liquids to produce fruit juices, coffee, tea, and whey in the food industry (67, 68, 71-74). Based

on previous studies, freeze crystallization can be considered as a method for wastewater treatment for municipal and industrial wastewater (75-79). A novel desalination method for seawater based on freezing has also been studied (80-82).

1.3 Research objectives

The main objectives of the thesis were the investigation of the potential application of freeze crystallization methods, i.e., layer freeze crystallization and suspension freeze crystallization, as concentration methods in the biorefinery field. Concentration based on freeze crystallization methods for aqueous sucrose solutions, aqueous [DBNH][OAc] ionic liquid solutions, ABE fermentation broths, and aqueous pyrolysis oil extract was investigated. Freeze crystallization was applied for the separation of 1-butanol from a two-liquid-phase system formed from feed aqueous ABE solutions. Cooling crystallization was used as a method for the recovery of levoglucosan from aqueous pyrolysis oil extract.
An overview of the crystallization methods investigated in the present work for various aqueous feeds relevant to bioprocessing is shown in Figure 1.

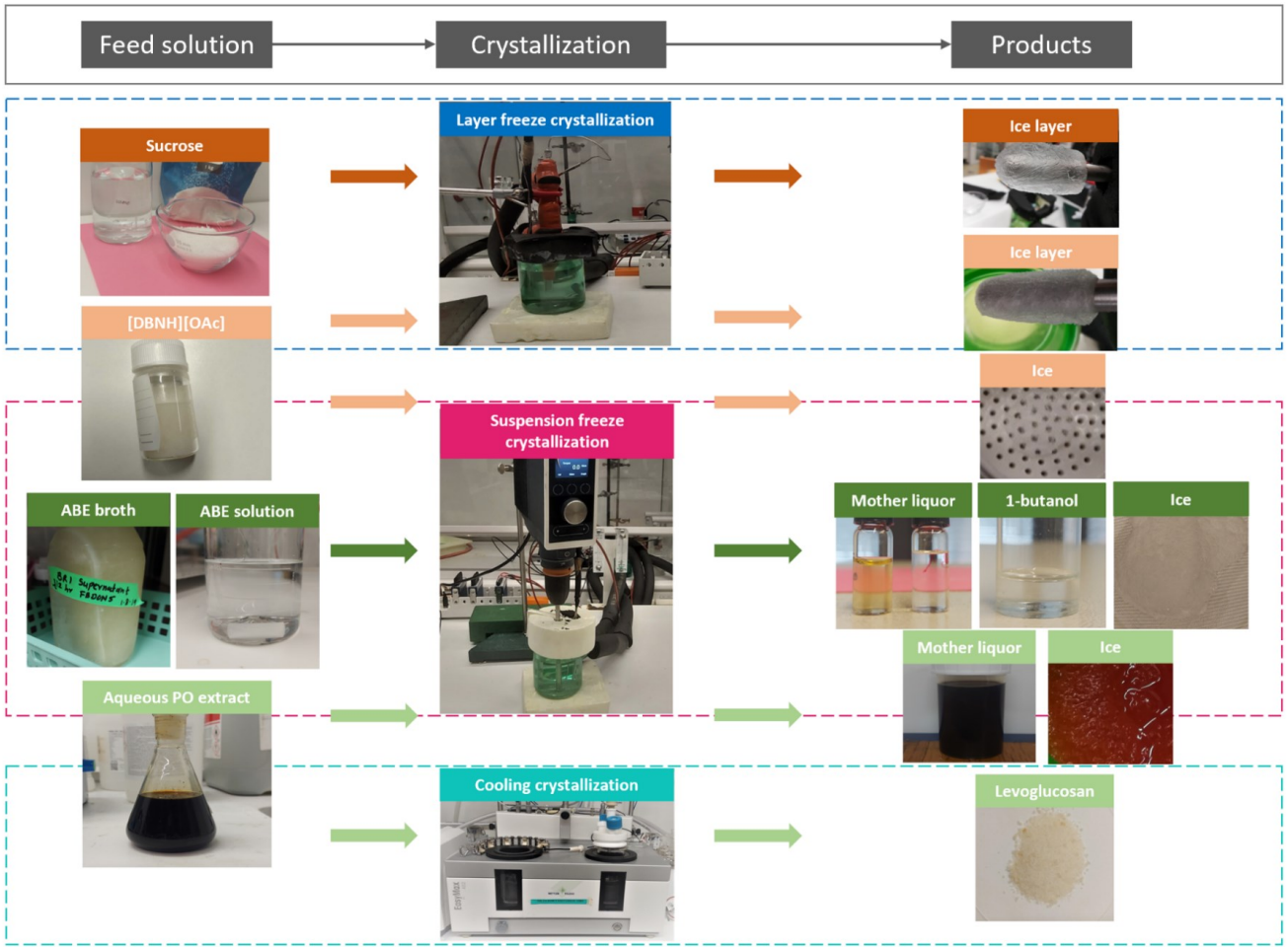

Figure 1. Freeze crystallization and crystallization from solutions applied for biorefinery system studies in the present work. (Dashed lines represent different crystallization methods applied, arrows indicate various feed solutions and corresponding products, photos illustrate the studied compound systems from different applications in an informative manner).

First, the experimental procedure for seeded layer freeze crystallization (LFC) on a cold finger was developed. The washing and melting steps of the formed ice layers were also determined. The heat transfer phenomenon in layer freeze crystallization studies was investigated numerically using computational fluid dynamics (CFD) simulation.
Second, a seeded suspension freeze crystallization (SFC) system with a scraper was designed. Procedures for ice separation, washing, and melting were also developed.

The research, discussed in the following sections, can be grouped into the following categories:

1. Freeze crystallization thermodynamics in terms of solid-liquid equilibrium and aqueous solution ideality was investigated by means of freezing point measurements and calculations of water activity coefficient.
2. Ice crystallization kinetics was investigated based on determined nucleation rates and measured overall crystal growth rates.
3. Freeze crystallization separation efficiency was assessed with determined distribution coefficients and ice yields.
4. Mother liquor concentrations and ice crystals purities were determined by different analytical methods.
5. Numerical study on heat transfer prior to layer freeze crystallization of aqueous sucrose solutions with different viscosity was conducted with CFD simulations.
6. 1-butanol was separated in the form of a 1-butanol enriched phase formed due to ABE solution concentration. 1-butanol yield and purity were investigated.
7. Levoglucosan was recovered by cooling crystallization and crystals were characterized (shape, particle size distribution, polymorphism).

2. Experimental Methodology

As discussed in the introduction section, the methodology for suspension and layer freeze crystallization experiments was developed during this thesis work. This section focuses on an explanation of these methods and how they were applied for various solutions.

2.1 Aqueous solutions studied

The freeze crystallization experiments were performed on various aqueous solutions. In this chapter, aqueous solutions are categorized into two groups: synthetic solutions and biorefinery process solutions. Synthetic solutions were prepared by dissolving commercial organic compounds in water. Biorefinery process solutions is a term related to aqueous PO extract and ABE fermentation broths.

The synthetic aqueous solutions were sucrose solutions, [DBNH][OAc] ionic liquid solutions, 1 butanol solution, and ABE solutions. The above-mentioned aqueous solutions were prepared by dissolution of appropriate solute(s) in ultrapure Millipore water and then mixed with a magnetic stirrer for an hour at 380 rpm.

The [DBNH][OAc] ionic liquid was a hygroscopic compound and a certain amount of it was measured out inside a glow box (relative humidity lower than 0.001 %) before adding water and mixing the solution outside. In the case of ABE solution preparation, acetone, 1-butanol, and ethanol were mixed with water inside an enclosed Wheaton Celstir double sidearm spinner flask to minimize solvent evaporation.

The exact compositions of the various synthetic aqueous solutions are given in Table 1.

Table 1. Compositions of aqueous solutions.

Aqueous solution	Solute, wt.%	Solute, mol/kg$_{(water)}$	Water, wt.%
Sucrose	10	$3.25 \cdot 10^{-4}$	90
	23	$8.73 \cdot 10^{-4}$	77
	30	$1.25 \cdot 10^{-3}$	70
[DBNH][OAc]	3	$1.68 \cdot 10^{-4}$	97
	6	$3.46 \cdot 10^{-4}$	94
1-butanol	8	$1.17 \cdot 10^{-3}$	92
ABE	3:8:1	0.59:1.23:0.25	88
	6:16:2	1.36:2.84:0.57	76
	10:17:2	2.42:3.23:0.61	72

The aqueous PO extract was separated from pyrolysis oil produced from pinewood chips by slow pyrolysis. The 1:1 and 1:5 PO extracts were obtained in liquid-liquid extraction with the addition of water to pyrolysis oil in water: pyrolysis oil ratios of 1:1 and 1:5 (mass based). The water content in the 1:1 PO extract and 1:5 PO extract was 77.7% and 91.6%, respectively. The major compounds in the pyrolysis oil were levoglucosan, formic acid, and acetic acid. The minor compounds were carbonyls, phenols, and furans. ABE fermentation broths were produced by fermentation of glucose with a bacterial strain - Clostridium acetobutylicum, and usage of L-cysteine as a reducing agent. The fermentation broth contained 96% water. Alongside acetone, 1-butanol and ethanol organic acids (acetic and butyric) were minor compounds present in the ABE fermentation broth. The main compounds present in the original pyrolysis oil and ABE fermentation broths are given in Table 2.

Table 2. Compositions of PO and ABE fermentation broths.

Solution	Organic compounds	Mass based, %
1:5 PO extract	Levoglucosan	1.66
	Formic acid	3.627
	Acetic acid	1.135
ABE fermentation broth 1	Acetone	0.904
	1-Butanol	1.686
	Ethanol	0.165
ABE fermentation broth 2	Acetone	0.918
	1-Butanol	1.683
	Ethanol	0.169

2.2 Suspension freeze crystallization

The suspension freeze crystallization experiments were conducted inside a 250 mL glass jacketed crystallizer closed with a polystyrene cap and connected to a thermostat (Lauda ECO RE1050). A crystallizer with an inner and outer diameter of 70 mm and 90 mm, respectively, and a height of 80 mm was used. The coolant was an aqueous 50 vol.% ethylene glycol mixture circulating through the jacketed crystallizer at flow rate of 1.64 L/min. The suspension freeze experiments were performed on the following aqueous solutions: [DBNH][OAc] ionic liquid solutions, pyrolysis oil (PO) extract, 1-butanol solutions, acetone-1-butanol-ethanol solutions, and ABE fermentation broths. The ice crystallization was initiated with ice crystal seeding when the temperature of the solution reached a stable undercooling temperature. The solutions were stirred at 18 rpm throughout the process with a stirrer, with the main purpose of preventing ice formation on the walls of the crystallizer. Stirrer was an anchor type impeller with tip speed of $6.6 \cdot 10^{-2}$ m/s and mixing Reynolds number of 2576 (calculated for water at 0 °C). Suspension freeze crystallization (SFC) was performed by a one-step and two-step method. Two-step SFC was performed for ABE fermentation broths and aqueous PO extract solutions to further enhance the concentration of these feed solutions. The scheme of the experimental setup is shown in Figure 2.

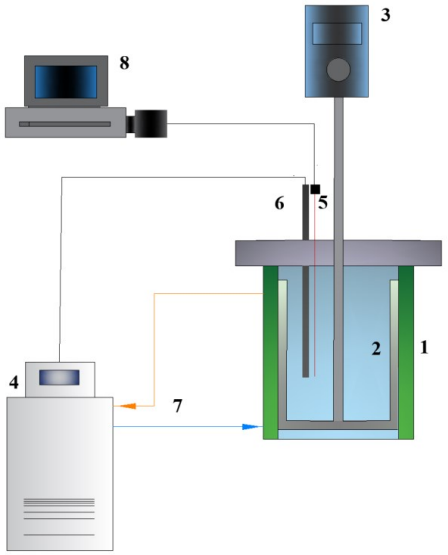

Figure 2. Suspension freeze crystallization setup: 1. crystallizer, 2. scraper, 3. mixer, 4. thermostat, 5. thermocouple, 6. Pt-100, 7. jacket coolant circulation, 8.data acquisition. Reprinted with permission from Paper 1. Copyright 2020 the authors, published by the MDPI.

Ice crystals formed from aqueous pyrolysis oil (PO) extract and aqueous 1-butanol solutions are shown in Figure 3.

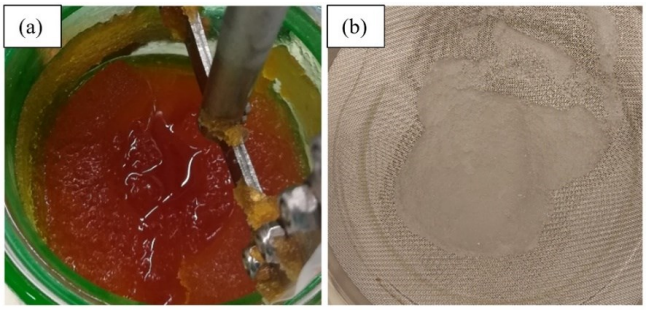

Figure 3. Ice samples: (a) Ice and mother liquor produced from PO extract solutions, (b) Ice formed from aqueous 8 wt.% 1-butanol solution separated from mother liquor.

After SFC, the formed ice crystals were separated from mother liquor on sieve. Approx. 25 g of ice was sampled out and washed with zero-degree Millipore water and then melted. Purity of melted ice sample and concentration of mother liquor were determined by various analytical methods discussed in section *2.4: Analytical methods*.

2.3 Layer freeze crystallization

Layer freeze crystallization experiments were performed by immersing a cold finger in the same crystallizer that was used for suspension freeze crystallization. The cold finger was

connected to another thermostat (Lauda ECO RE1050) that circulated coolant at a flow rate of 0.54 L/min. The temperature data for the inlet coolant, outlet coolant, and coolant inside the cold finger were recorded. The layer freeze crystallization experiments were performed on aqueous sucrose and aqueous [DBNH][OAc] solutions in static mode. An ice layer was formed from the aqueous solution on the surface of the undercooled cylindrical cold finger immersed inside the crystallizer vessel. The diameter of the cold finger was 10 mm and the cooling length available for a layer to form on was 40 mm. The seeding was performed by attaching an ice crystal to the under surface of the cold finger. The experimental setup is shown in Figure 4.

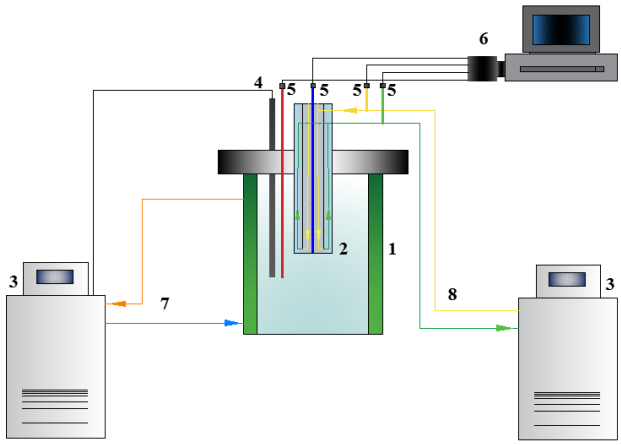

Figure 4. Layer freeze crystallization setup: 1. crystallizer, 2. cold finger, 3. thermostat, 4. Pt-100, 5. thermocouples, 6. data acquisition 7. jacket coolant circulation, 8. cold finger coolant circulation. Reprinted with permission from Paper 1. Copyright 2020 the authors, published by the MDPI.

The growing ice layer, two minutes and four minutes after seeding for the [DBNH][OAc] and sucrose solutions, respectively, are shown in Figure 5. The ice layers formed after 40 minutes of crystallization are also presented.

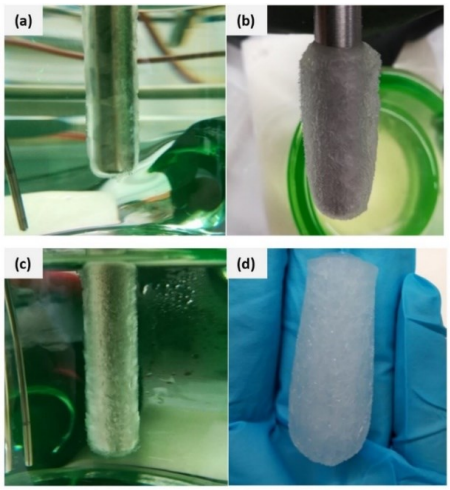

Figure 5. Ice layers formed from aqueous solutions: (a) 3 wt.% [DBNH][OAc] after 2 min of freezing (ΔT= 1.23 °C), (b) 3 wt.% [DBNH][OAc] after 40 min of freezing, (c) 23 wt.% sucrose after 4 min of freezing (ΔT= 1.07 °C), (d) 23 wt.% sucrose after 40 min of freezing (ΔT= 1.07 °C).

2.4 Analytical methods

The aqueous solutions concentrated by freeze crystallization contained different organic solvents, as discussed in the previous section: *2.1 Studied aqueous solutions*. The ice crystals that were produced contained impurities and inclusions related to the solutes present in the feed aqueous solution. Investigation of ice purity, i.e., determining the concentration of impurities present in washed ice samples, is necessary in order to obtain information on freeze crystallization efficiency based on the ice yields and distribution coefficient; this is discussed in more detail in section *4.2: Separation efficiency*. Depending on the feed aqueous solutions, different analytical methods were used to determine the quantity of impurities present in the ice produced. Similarly, the concentration of solutes in the remaining mother liquor was determined.
An overview of various analytical methods and instruments used to perform the analyses is given in Table 3.

Table 3. Analytical methods with corresponding list of instruments used to characterize ice and mother liquor.

Aqueous solution	Ice	Mother liquor	Instrument(s)
Sucrose	Refractive index	Refractive index	Dr. Kernchen Abbemat digital refractometer
[DBNH][OAc]	Electrical conductivity	Electrical conductivity	Consort C3050 PH/EC meter
1-butanol and ABE solutions	Total organic content (TOC)*	Gas chromatography (GC)**	*Shimadzu TOC-VCPH **Shimadzu GC-2010 Plus
ABE fermentation broths	Total organic content (TOC)	-	Shimadzu TOC-VCPH
Aqueous PO extract	Total organic content (TOC)*	High-performance liquid chromatography (HPLC)**	*Shimadzu TOC-VCPH **Shimadzu SIL-20 series HPLC

Moreover, the compositions of the organic compounds present in the ABE fermentation broths were determined based on HPLC (Paper 3) and the compositions of the aqueous PO extract were determined by HPLC and GC (Paper 4). The amount of water in the feed PO extract solutions and mother liquors was determined by Karl-Fischer titration.

3. Thermodynamics of freeze crystallization

The freezing points determined based on the suspension freeze crystallization experiments, the phase transition phenomena investigated by DSC, and solution ideality are presented in the following sections.

3.1 Freezing points of aqueous solutions

The binary phase diagram below shows the presence of different phases of two compounds as a function of their composition in the given temperature range. Therefore, the theoretical crystal yield of the crystalline compound in a certain temperature range can be calculated based on the phase diagram data. The solid-liquid equilibria of the water-ionic liquid (IL) compound system were investigated using DSC 3 Mettler Toledo scanning calorimetry (DSC). Two types of ionic liquids were studied, namely [DBNH][OAc] and [mTBDH][OAc]. Details of the DSC analysis of the water - [DBNH][OAc] ionic liquid system are given in Paper 1. Samples of the water - [mTBDH][OAc] ionic liquid mixtures were cooled down to -80 °C and then heated up to +90 °C with cooling and heating rates of 5 °C/min during DSC analysis.
The phase diagrams of the water - [DBNH][OAc] ionic liquid and water - [mTBDH][OAc] ionic liquid compound systems are shown in Figure 6.

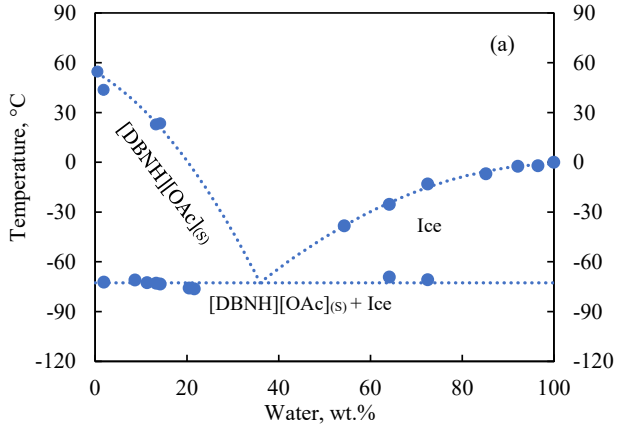

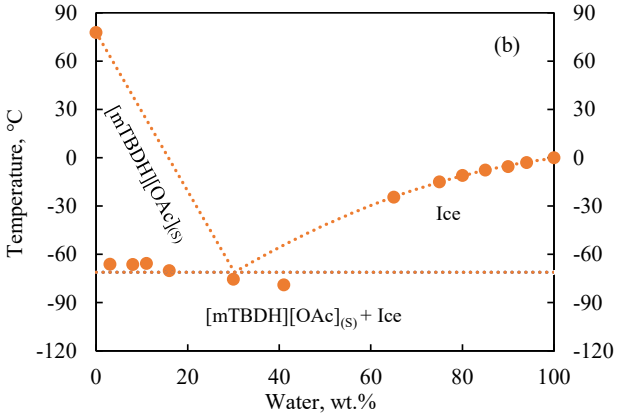

Figure 6. Phase diagrams for (a) water - [DBNH][OAc] compound system, (b) water - [mTBDH][OAc] compound system.

Based on the phase diagrams, the melting points of [DBNH][OAc] ionic liquid and [mTBDH][OAc] ionic liquid are 54.5 °C and 77.8 °C, respectively. For the [mTBDH][OAc] ionic liquid samples that contained water in the range of 3 wt.% to 41 wt.%, only glass transitions were observed upon heating. The phase transitions of samples that contained 50 wt.% and 54 wt. % of water were not noticeable on the DSC thermogram. The samples with higher water concentration, from 65 % to 100 %, underwent phase transitions upon cooling and heating where crystallization and melting peaks were observed for the water phase. Hence, the data obtained on the melting temperatures were used for the ice curve plot. Similar phase transition phenomena related to the ionic liquid-enriched regions and water-enriched regions were observed for the water - [DBNH][OAc] ionic liquid mixtures (Paper 1). The eutectic point for the water - [mTBDH][OAc] ionic liquid systems was estimated to be -71 °C (30 wt.% water), which is close to the eutectic point of -73 °C (36 wt.% water) for the water - [DBNH][OAc] ionic liquid system.

The low eutectic points and tendency of ionic liquids to form amorphous structures from ionic liquid-enriched samples were the main reasons why melt crystallization was not considered as a purification method for ionic liquid. Consequently, freeze crystallization was studied as a method to concentrate aqueous [DBNH][OAc] ionic liquid solution.

The freezing points of different aqueous solutions were determined by means of suspension freeze crystallization experiments. A typical cooling curve obtained based on recorded temperature data during suspension freeze crystallization is shown in Figure 7.

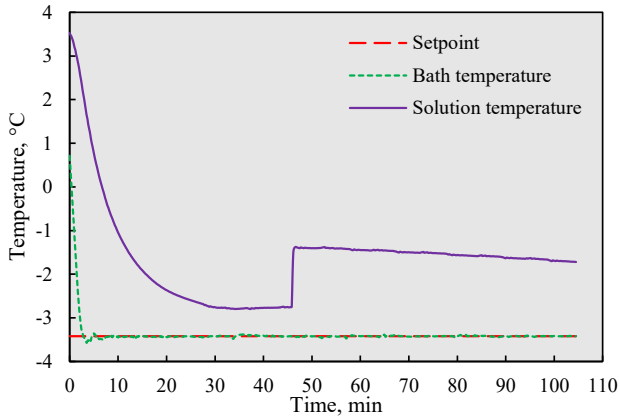

Figure 7. Measured temperatures for 6 wt.% [DBNH][OAc] ionic liquid solution for 60 minutes of crystallization.

The cooling curve shows the solution temperature change during cooling, ice seeding, and crystallization based on acquired and stored temperature data. The cooling of the solution proceeded until the solution temperature reached a constant undercooling temperature. Ice seeding was then performed, and an immediate rise of temperature was evident as the latent heat of crystallization was released and the solution temperature reached its freezing point. As crystallization progressed further, the solution temperature dropped as the solution became more concentrated. The amount of ice could be large for a significant undercooling degree, which could lead to increased solution concentration. Consequently, this means that the measured temperature is slightly lower than the freezing point of the initial solution. Additionally, process curves for the set temperature and coolant temperature inside the thermostat bath are shown to highlight that the process temperature was controlled with the thermostat's internal Pt-100 thermometer. Table 1 shows a summary of the freezing points of the different feed solutions that were studied.

Table 4. Freezing points of aqueous solutions.

Aqueous solution, mass based	Freezing point, °C
3 wt.% [DBNH][OAc] IL	-0.62 ± 0.01
6 wt.% [DBNH][OAc] IL	-1.29 ± 0.02
1:1 PO extract	-4.97 ± 0.24
1:5 PO extract	-1.40 ± 0.28
1:10 PO extract	-0.93 ± 0.04
3:8:1:88 ABEW	-3.70 ± 0.03
10:17:2:71 ABEW	-7.51 ± 0.07
6:16:2:76 ABEW	-5.95 ± 0.22
8 wt.% 1-butanol	-2.12 ± 0.03
ABE fermentation broth 1	-0.56
ABE fermentation broth 2	-0.73

3.2 Solution ideality

The intermolecular interaction between solvent and solute molecules is related to the ideality of the solution. Negligible intermolecular attraction or repulsion indicates that the solution is ideal, whereas attractive or repellent forces between molecules are direct indicators that the solution is non-ideal. This is represented quantitatively with activity coefficient (γ).
Water activity coefficients for aqueous solutions were determined based on the Van't Hoff equation (83). The water activity coefficients (γ) as a function of the solute mole fraction (χ) are presented in Figure 8.

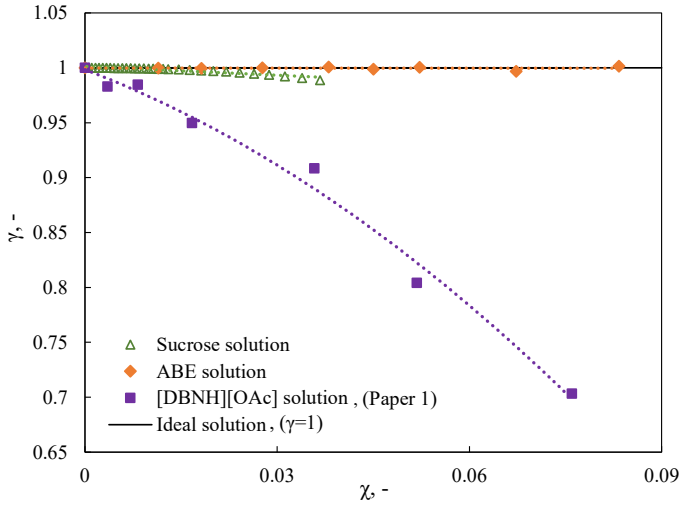

Figure 8. Water activity coefficient for different aqueous solutions.

Based on Figure 8, the aqueous ABE solutions and aqueous sucrose solutions are ideal. The aqueous [DBNH][OAc] solutions are non-ideal solutions exhibiting attractive intermolecular forces (γ < 1) (Paper 1). The aqueous pyrolysis oil extract solutions studied were very complex mixtures of various organic compounds. Hence, the water activity coefficients were estimated for model aqueous PO extract solutions consisting of three major organic compounds present in real PO extract, i.e., levoglucosan, formic acid, and acetic acid, neglecting the rest of the organics that contributed only a few percentage points to the total composition. The modeled PO extract solutions were ideal solutions (γ = 1) in a solute mole fraction range from 0.017 to 0.03, and with experimentally determined freezing points in a range of -1.38 °C to -1.88 °C.
The information on ideality of solution is one of the parameters used to explain the differences in ice crystallization kinetics formed from different solutions. Other parameters are the initial water content in feed solutions and the applied range of undercooling degrees.

4. Kinetics of freeze crystallization

The overview and comparison of ice crystallization kinetics and freeze crystallization separation efficiency for various aqueous solutions are presented in the following sections.

4.1 Ice nucleation rate and overall crystal growth rate

The nucleation rate of a single ice crystal was determined with the model proposed by Shirai et al. (96). Their model is based on the temperature response method. The temperature response method is the determination of the maximum temperature slope of the cooling curve part where a temperature change caused by the release of latent heat of crystallization is observed upon ice seeding. The information on determined nucleation rates with data obtained from batch suspension freeze crystallization is important for the design of a continuous crystallization process because the nucleation rate is inversely proportional to the residence time.

The nucleation per ice crystal, β, is expressed by the following equation:

$$\boldsymbol{\beta}\left[\mathbf{s}^{-1}\right] = \mathbf{5.93} \cdot \frac{\left(\boldsymbol{\mu}_2^{\mathbf{0}}\right)^{\mathbf{0.027}}}{\boldsymbol{\Delta T}[\mathbf{K}]} \cdot \left(\frac{\boldsymbol{dT}[\mathbf{K}]}{\boldsymbol{dt}[\mathbf{s}]}\right)_{\boldsymbol{max}} \qquad (1)$$

where ΔT is the undercooling degree, $(dT/dt)_{max}$ is the maximum slope of the temperature response curve, and μ^o_2 is the second moment of ice seed crystal distribution. In the equation, the term of second moment of ice seed crystal distribution is considered to be unity. Ice nucleation rate for various studied solutions in shown in Figure 9.

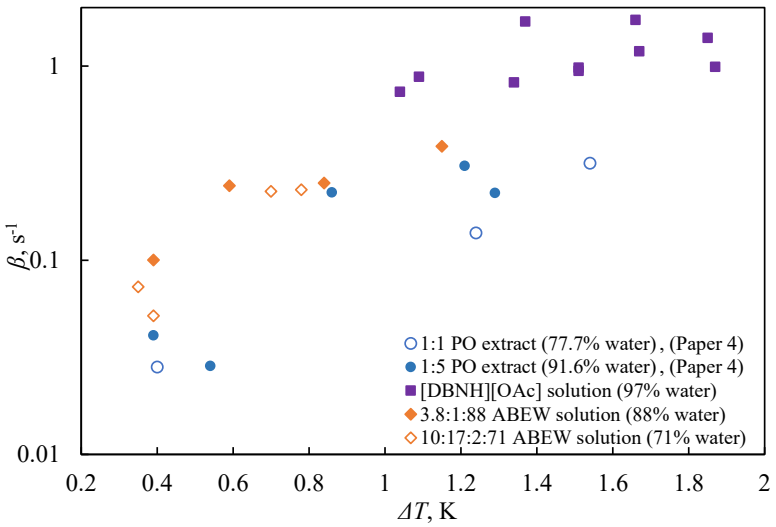

Figure 9. Nucleation rate per crystal for different aqueous solutions.

In Figure 9, it is apparent that nucleation occurs the fastest for aqueous [DBNH][OAc] solutions, even though the solutions are non-ideal with attractive intermolecular forces. The reason is that [DBNH][OAc] solutions initially contained the highest amount of water, and the undercooling degree range applied, which is the driving force of freeze crystallization, was higher in comparison with the other solutions. The slowest ice nucleation is observed for PO extract solutions. For a similar range of undercooling degrees, nucleation occurred faster for ABE solutions in comparison with PO extract, although the initial water content was lower in the 3:8:1:88 and 10:17:2 ABEW solutions than in the 1:5 PO and 1:1 PO extracts, respectively. Therefore, in the case of continuous freeze crystallization, the shortest residence time and smaller crystallizer volume are needed for PO extract solutions followed by ABE solutions and aqueous [DBNH][OAc] solutions.

The overall mass ice growth rate, $R_{G,ice}$ is determined based on the mass and surface area of ice crystals formed during a certain freezing time and is expressed by Equation (2):

$$\boldsymbol{R_{G,ice}[\mathrm{kg}\cdot\mathrm{m}^{-2}\cdot\mathrm{s}^{-1}] = \frac{m_{ice}[\mathrm{kg}]}{A[\mathrm{m}^2]\cdot t[\mathrm{s}]}} \qquad (2)$$

The overall ice growth rates as a function of applied undercooling degree are determined for ice samples formed from different aqueous solutions by means of suspension and layer freeze crystallization experiments. In Figure 10, the overall ice growth rates are shown for ice formed by suspension freeze crystallization.

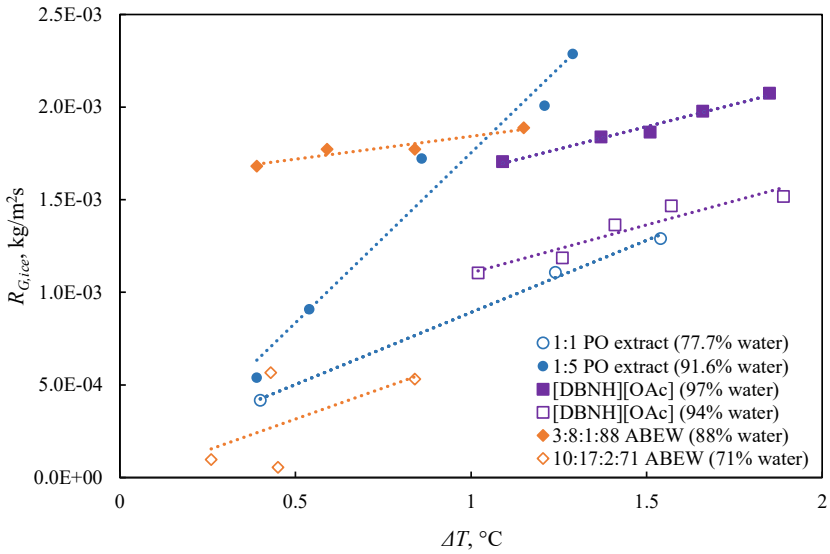

Figure 10. Overall ice growth rates as a function of undercooling degrees for ice crystals obtained from different aqueous solutions by suspension freeze crystallization.

The overall growth rates for different ice crystal samples were in the range of 10^{-5} - 10^{-3} kg·m^{-2}·s^{-1} for undercooling degrees in the range of 0.26-1.89 °C. Ice growth for 3:8:1:88 ABEW progressed the fastest at range of lower undercooling degrees and it is comparable with growth rates of ice crystals formed from 3 wt.% [DBNH][OAc] with higher undercooling degrees. However, the ice growth rates were the lowest for 10:17:2:71 ABEW in comparison with the growth rates related to other solutions. The 10:17:21:71 ABEW solution had the lowest initial water amount, and was a unique solution in comparison with the other solutions, because ice was formed in a two-liquid phase system, i.e., a 1-butanol phase and a water-enriched phase, which may affect the ice growth kinetics. Overall ice growth rates for 1:5 PO extract solution, as the most complex type of organic solution, changed more significantly at applied range of undercooling degrees. Ice growth from aqueous 1:1 PO extract solutions progressed at moderate rates, comparable with the 6 wt.% [DBNH][OAc] solutions for similar range of undercooling degrees.

The ice growth rates of ice layers formed by layer freeze crystallization from aqueous sucrose and [DBNH][OAc] solutions are shown in Figure 11.

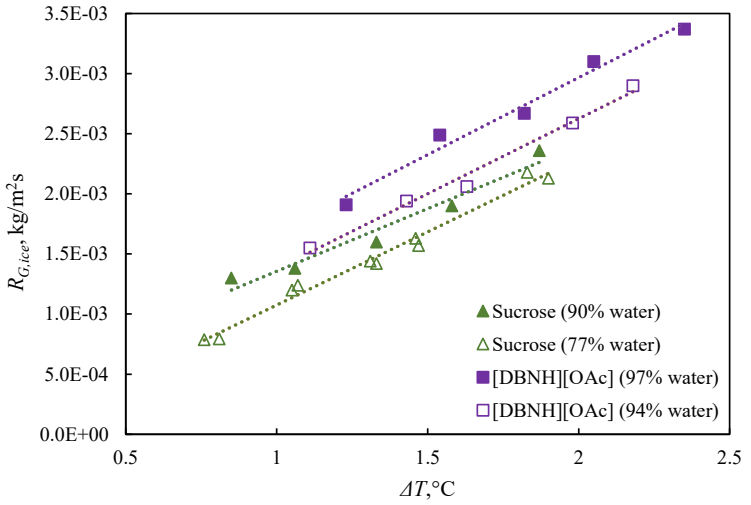

Figure 11. Overall ice growth rates as a function of undercooling degrees for ice crystals obtained from different aqueous solutions by layer freeze crystallization.

The formation of ice layers from the aqueous sucrose and [DBNH][OAc] solutions occurred with very similar growth kinetics for a range of undercooling degrees from 0.76 °C to 2.35 °C. In Figure 11, there is very good correspondence between the initial water content and the overall ice growth rates. Hence, ice layer growth kinetics tend to increase with a higher initial water content. Even though the 23 wt.% solution has high viscosity and a significantly lower initial water content than the other solutions, its ice layer growth kinetics are comparable with the growth kinetics of other solutions, i.e., sucrose and [DBNH][OAc] solutions. First, the explanation for this phenomenon may lie in the nature of sucrose solutions, which are ideal with no drastic difference between the freezing points of 10 wt.% sucrose solution (-0.63 °C) and 23 wt.% sucrose solution (-1.78 °C); consequently undercooling as a driving force is comparable. Second, [DBNH][OAc] solutions have slightly faster growth kinetics with a much higher water content than 10 wt.% sucrose solution, because [DBNH][OAc] solutions are non-ideal solutions with attractive intermolecular forces.

4.2 Separation efficiency

The efficiency of freeze crystallization applied as a concentration method for various aqueous solutions is determined by two parameters: ice yield and distribution coefficient. Freeze crystallization should result in relatively high production of ice with a high purity level (low concentration of impurities (solutes)). Therefore, ice yield, Y, is expressed as a percentage of the ratio of the masses of pure ice produced and initial water. Whereas the distribution coefficient, K, is related to ice purity and is the ratio of the concentration of impurities (solutes) in washed ice and the initial concentration of solutes present in the feed solution.
The expressions for ice yield and distribution coefficient are given by Equations (2) and (3):

$$Y[\%] = \frac{m_{ice,pure}[\mathbf{kg}]}{m_{water,feed}[\mathbf{kg}]} \cdot \mathbf{100} \qquad (2)$$

$$K[-] = \frac{C_{solute,ice}[\mathbf{wt.\%}]}{C_{solute,feed}[\mathbf{wt.\%}]} \qquad (3)$$

Ice yields related to different aqueous solutions are compared for freeze crystallization experiments performed with the same freezing times. Ice yields obtained from different aqueous solutions by suspension freeze crystallization for 60 and 80 minutes of freezing are shown in Figure 12.

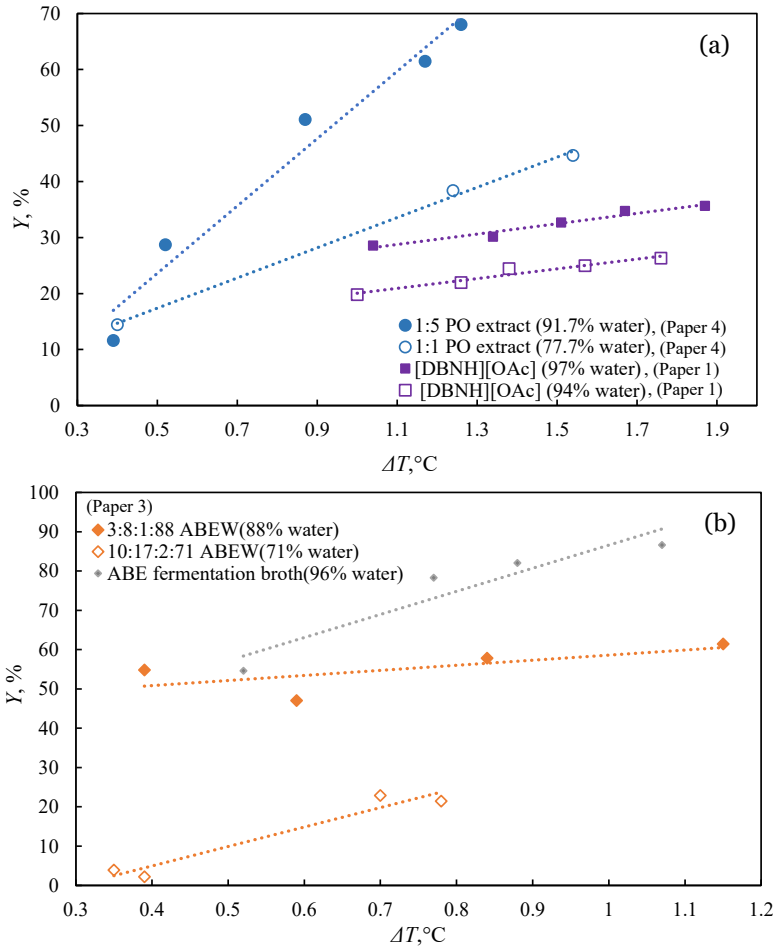

Figure 12. Ice yields obtained from various aqueous solutions by suspension freeze crystallization for freezing times of (a) 60 min and (b) 80 min.

In Figure 12(a), it is apparent that ice yields obtained from both aqueous PO extracts and both types of [DBNH][OAc] solution for 60 minutes of freezing by suspension freeze crystallization

have the expected tendency to increase with a higher initial water content of solution when there is an increase in undercooling degrees. The aqueous PO extracts have the lower initial water contents yet the higher ice yields at similar undercooling degrees in comparison with [DBNH][OAc] solutions. Whereas ice yields obtained from synthetic ABE solutions and ABE fermentation broths for 80 minutes of freezing (Paper 3), as expected, depend on the feed water content, with average ice yields values of 12.6%, 55.3%, and 75.4% for 10:17:2:71 ABEW, 3:8:1:88 ABEW, and ABE fermentation broth, respectively (Figure 12(b)).
Ice yields for aqueous sucrose and [DBNH][OAc] ionic liquid solutions investigated by layer freeze crystallization for freezing times of 40 and 60 minutes are presented in Figure 13.

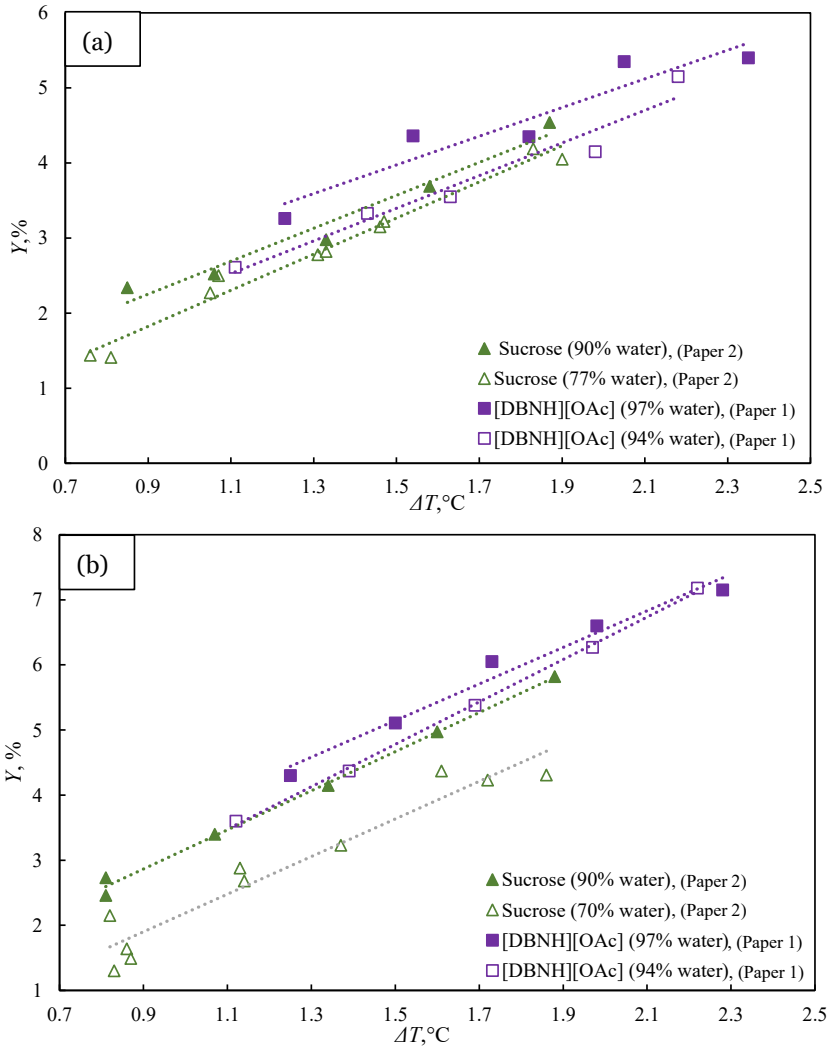

Figure 13. Ice yields obtained from various aqueous solutions by layer freeze crystallization for freezing times of (a) 40 min and (b) 60 min.

Based on Figure 13, the ice yields of ice layers formed from aqueous sucrose and [DBNH][OAc] solutions for 40 and 60 minutes of freezing have a common trend related to the initial water

content of the solution and the applied undercooling degree, similarly to what was observed and discussed in the case of suspension freeze crystallization.

The distribution coefficients for ice formed from aqueous ABE solution, ABE fermentation broth, and 1:5 PO extract solutions by suspension freeze crystallization were very low, which is an indicator that the ice obtained was of high purity. The average distribution coefficient values for the above-mentioned solutions were in the order of 10^{-3} and less. The concentration of impurities present in washed and melted ice samples was determined based on TOC analysis (Table 2) and the average TOC was in the range of 4.5 – 953 ppm. However, ice crystals obtained from 3 wt.% and 6 wt.% [DBNH][OAc] solutions had average distribution coefficient values of 0.26 and 0.23, respectively. The distribution coefficient values of [DBNH][OAc] solutions differ in comparison with other aqueous solutions because different analytical methods were used to analyze ice purity, and ice crystal samples of a similar mass were washed with less water in the case of the former solutions and consequently may have resulted in more impure ice samples. The average distribution coefficient values for the range of applied undercooling degrees (0.76 - 2.35 °C) for ice layers formed from aqueous sucrose and [DBNH][OAc] solutions are given in Figure 14.

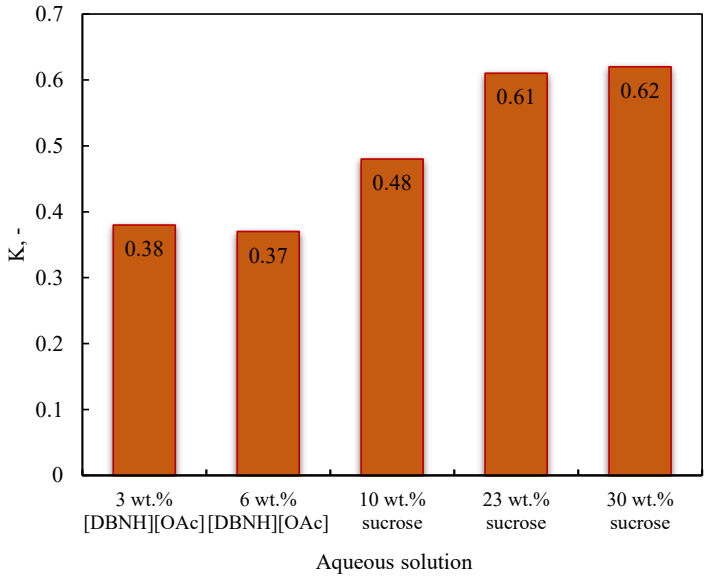

Figure 14. Average distribution coefficient for ice samples obtained from [DBNH][OAc] and sucrose solutions by layer freeze crystallization.

Based on the distribution coefficient values, it can be concluded that solute molecules were entrapped between the ice grains of ice layers and the washing step only removed the mother liquor from the surface of the layer. According to boundary layer growth theory, molecules of solutes (impurities) diffuse toward the surrounding mother liquor during ice layer formation (98). However, this process can be hindered if the ice layer growth rates are relatively high. For [DBNH][OAc] solutions, the distribution coefficient values increased with faster layer growth kinetics, whereas for sucrose solutions the distribution coefficients were almost

constant for the range of ice growth rates (Paper 1, Paper 2). Moreover, based on Figure 14, the distribution coefficients for [DBNH][OAc] solutions are lower than for sucrose solutions, even though the growth of ice layers from [DBNH][OAc] solutions proceeded slightly faster over the range of undercooling degrees applied, as shown in Figure 11. This is due to the fact that sucrose molecules are most likely trapped between ice grains, as diffusion from the forming ice layer is more difficult due to the higher viscosity of the surrounding undercooled solution and the larger size of the sucrose molecules.

4.3 Ice morphology

It has been reported previously that the shape of ice grains depends on the solutes present in the aqueous solution (97). The optical microscope images of ice crystals formed from different aqueous solutions by suspension freeze crystallization are shown in Figure 15. The images were taken with an Olympus BH-2 optical microscope at a magnification of 10x.

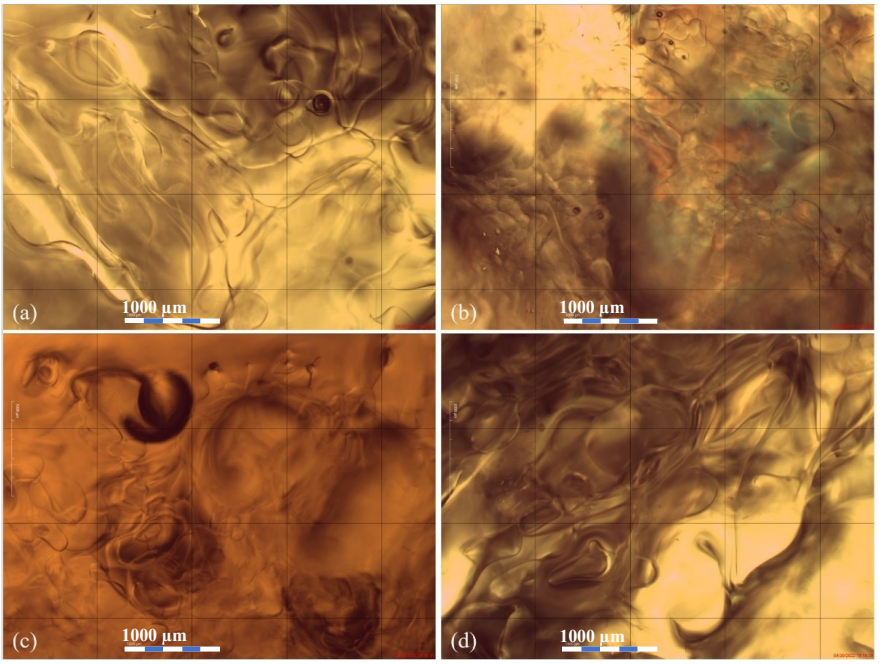

Figure 15. Images of unwashed ice crystals produced by suspension freeze crystallization from (a) 8 wt.% 1-butanol solution, (b) 3:8:1:88 ABEW solutions, (c) 1:5 PO extract, and (d) ABE fermentation broth 2 (magnification 10 X, bar scale 1000 µm).

Based on Figure 15, it is apparent that the ice crystals produced are quite large. Samples were not washed to reduce the time before optical microscope imaging at room temperature, as the ice samples melted easily. Even though, appropriate optical microscope parameters, such as magnification, were set prior to ice sample imaging to reduce imagining time, the melting of the ice samples was inevitable which is apparent in Figure 15. Entrapped mother liquor between ice crystals and some inclusions can be observed. Crystals obtained from 8 wt.% 1-butanol solution, 1:5 PO extract, and ABE fermentation broth are of comparable size, with some crystals as large as 1 mm. In the case of 3:8:1:88 ABEW, the crystals are smaller (≤ 0.5

mm) and mostly coin-shaped. The 3:8:1:88 ABEW solution has the highest concentration of organic compounds (total of 2.07 mol/kg(water) ABE solvents) in comparison with the ABE fermentation broth (0.466 mol/kg(water)), 8 wt.% 1-butanol solution (1.17·10-3 mol/kg(water)), and 1:5 PO extract (approx.1.15·10-3 mol/kg(water)). Hence, the relatively smaller ice crystals obtained from the 3:8:1:88 ABEW solution in comparison with the ABE fermentation broths may be the result of its higher ABE solvent concentration and the absence of other organic and inorganic compounds characteristic of ABE fermentation broths. In comparison with the 8 wt.% 1-butanol solution, it is apparent that the differences in ice morphology and size are a result of the influence of the acetone and ethanol present in the 3:8:1:88 ABEW solution.

5. CFD study on heat transfer

The heat transfer phenomena inside a crystallizer equipped with a cold finger prior to seeding and ice crystallization were investigated by CDF analysis using COMSOL Multiphysics software. The created geometries of the crystallizer vessel and cold finger were based on the actual dimensions of the crystallizer used for the layer freeze crystallization experiments. The coolant temperature circulating through the crystallizer jacket was the same as the solution freezing point; the cold finger temperature was set at two different undercooling temperatures to obtain undercooling degrees of 0.85 °C and 1.85 °C. The model solutions were based on 10 wt.%, 23 wt.%, and 30 wt.% sucrose solutions with corresponding thermophysical properties (density, viscosity, thermal conductivity, and specific heat transfer) that were defined in the model as temperature-dependent properties. The study obtained the temperature distribution of the solution when cooled down from 3 °C to its freezing point with certain undercooling degrees. In the case of stagnant aqueous solutions, heat is transferred via natural convection during the process of cooling down. The physical model used for CFD simulation was based on the integration of buoyancy-driven laminar flow and convective heat transfer (Publication 2). The heat fluxes, qi, transferred through the surfaces of the jacketed crystallizer and cold finger from the cooling solution are given by Equation (4):

$$\boldsymbol{q_i}[\mathbf{W \cdot m^{-2}}] = -\boldsymbol{U_i}[\mathbf{W \cdot m^{-2}K^{-1}}] \cdot (\boldsymbol{T}[\mathbf{K}] - \boldsymbol{T_i}[\mathbf{K}]) \qquad (4)$$

where: U_i is the overall heat transfer coefficient related to the jacket/cold finger, T is the time-dependent solution temperature, and T_i is the jacket/cold finger temperature. In Paper 2, equations and models were discussed for overall heat transfer coefficients that contained terms for the heat transfer coefficient of the coolant circulating through the jacket and cold finger. The overall heat transfer coefficient related to the cold finger was around six times higher than that for the crystallizer jacket. This is a direct result of the lower heat transfer resistance of the cold finger element due to the high thermal conductivity of stainless steel (cold finger material) and the high heat transfer coefficient of the coolant circulating through the cold finger related to its flow geometry. The heat transfer coefficients for the cold finger and jacket coolants were determined based on Nusselt numbers, which depend on the flow geometry and coolant thermophysical properties. Consequently, the coolant flow cross sections, annular for the cold finger and rectangular for the jacket, only affect the heat transfer coefficient, as the same type of coolant (ethylene glycol-water mixture) was used for both elements. A schematic representation of the coolant flow geometry for the crystallizer jacket and cold finger is shown in Figure 16.

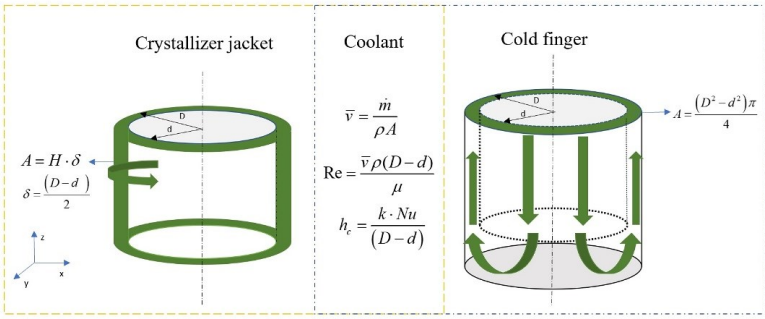

Figure 16. Flow geometry of coolants circulating through crystallizer jacket and cold finger.

The thermophysical properties of the aqueous sucrose solutions studied at their freezing points are given in Table 5.

Table 5. Thermophysical properties of 10 wt.%, 23 wt.% and 30 wt.% sucrose solutions at their freezing points.

Aqueous solution	Freezing point, °C	Dynamic viscosity, mPa·s	Density, kg·m^{-3}	Thermal conductivity, W·m^{-2}K^{-1}	Specific heat capacity, J·kg^{-1}K^{-1}
10 wt.% sucrose	-0.63	2.01	1041.6	0.545	3684
23 wt.% sucrose	-1.78	4.74	1098.4	0.498	3366.1
30 wt.% sucrose	-2.64	7.51	1131.85	0.476	3190.4

A study was made of how heat transfer during the cooling of various solutions is influenced by the thermophysical properties of the sucrose solutions, investigated as well as by the different cooling temperature ranges set based on the freezing point. Hence, two studies of the cooling of sucrose solutions were conducted: when the solutions were cooled down to their freezing point, and when they were cooled down to -1 °C. In both cases the undercooling degree was 0.85 °C. The temperatures obtained for the solutions as a function of time are shown in Figure 17.

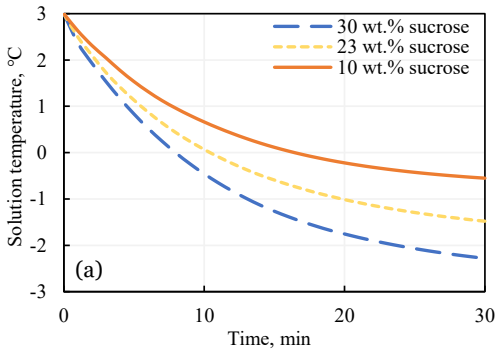

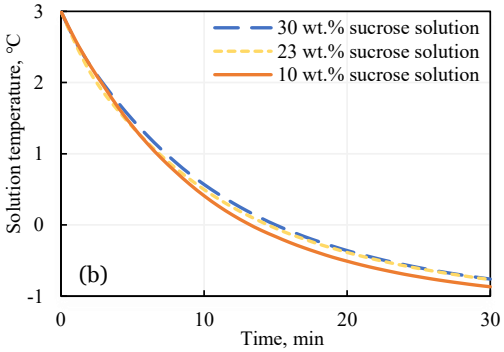

Figure 17. Cooling curves for aqueous sucrose solutions for 30 minutes of cooling (a) to solution freezing point (b) to -1°C with the same undercooling degree of 0.85 °C.

Based on the modeled cooling curves (Figure 17(a)), when solutions are cooled down to their freezing point, cooling proceeds at a higher rate for solutions with a lower freezing point (more concentrated solution), because the cooling time (60 min) set for the CFD simulation was the same for all solutions. The first 30 minutes of the cooling are shown in Figure 17(a). Even though 30 wt. % sucrose solution cools faster than 23 wt.% and 10 wt.% sucrose solutions, it needed the longest time before its temperature reached freezing point and the solution became undercooled (supersaturated), as described in Publication 2. Therefore, when the solutions were cooled down in the same cooling range (from +3 to -1 °C) for 30 minutes, the differences in cooling kinetics were purely the result of their thermophysical properties (Figure 17(b)). The colored graphs of overall temperature distributions for sucrose solutions at their respective points of cooling when they became undercooled are shown in Figure 18.

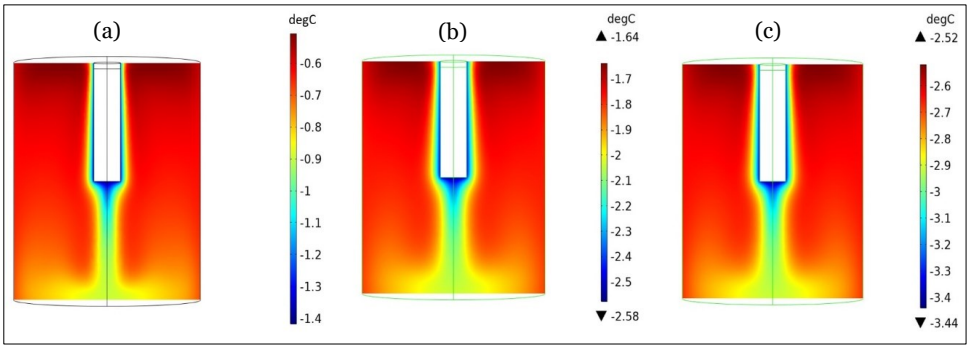

Figure 18. Temperature distribution for (a) 10 wt.% sucrose at the 36th minute, (b) 23 wt.% sucrose at the 47th minute and (c) 30 wt.% sucrose at the 50th minute of cooling for undercooling degree of 0.85 °C.

23 wt.% and 30 wt.% sucrose solutions needs 11 and 14 minutes more of cooling to became undercooled (supersaturated) when compared with 10 wt.% sucrose solution for undercooling degree of 0.85 °C. The convective heat transfer coefficient, h, for different solutions is determined as a time-dependent parameter based on the heat fluxes and temperature differences between the solution bulk temperature and cooling surface temperature.

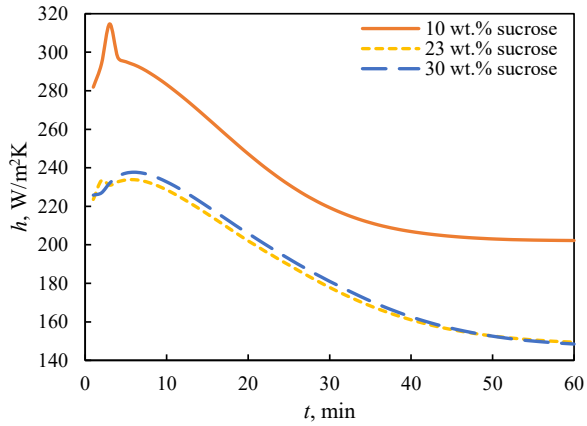

Figure 19. Convective heat transfer coefficients for solutions at cold finger surface, undercooling of 0.85 °C.

The convective heat transfer coefficients are significantly higher for 10 wt.% sucrose solution than for 23 wt.% and 30 wt.% sucrose solutions. Therefore, heat transfer caused by natural convection is more intensive for solution of lower density. In general, the convective heat transfer coefficient decreases notable as the difference between bulk temperature and cold finger temperature gets smaller and solution become undercooled.

Temperature distribution curves of aqueous sucrose solutions along vertical central axis, z, for 30 minutes of cooling and undercooling degree of 0.85 °C are shown in Figure 20.

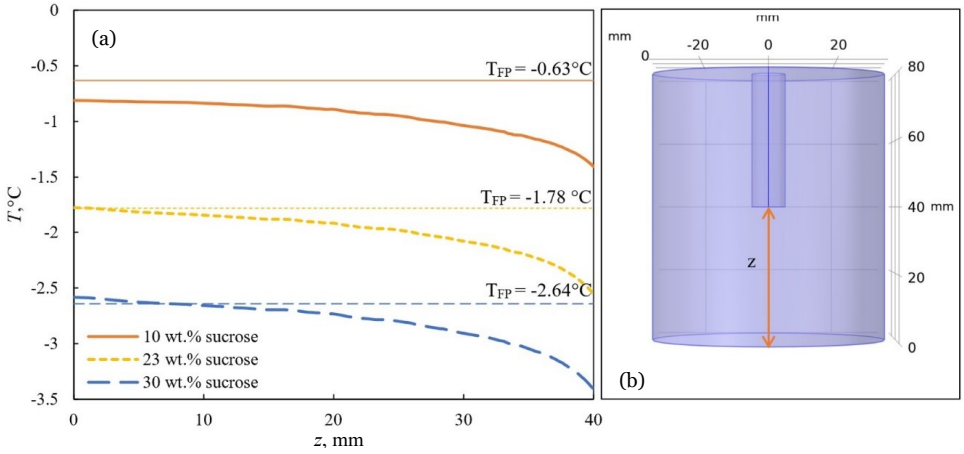

Figure 20. (a) Temperature distribution along vertical axis for sucrose solution for 30 minutes of cooling and undercooling of 0.85°C and (b) position of vertical central axis – z inside crystallizer equipped with cold finger.

For the crystallizer region that occupies volume under cold finger towards the bottom of crystallizer, along the vertical central axis, 10 wt.% sucrose and 23 wt.% sucrose solution are fully undercooled. 30 wt.% sucrose solution is not undercooled just in narrow region, approx. at distance of 7 mm from the bottom of the crystallizer. More comprehensive studies on

temperature distribution and thermal boundary layer for undercooling degrees of 0.85 °C and 1.85 °C are presented in Paper 2.

6. 1 – butanol separation from synthetic ABE solutions

The separation of 1-butanol from aqueous ABE solutions (3:8:1:88, 6:16:2:76, and 10:17:2:71 ABEW, (mass based)) was enabled by suspension freeze crystallization, because 1- butanol is sparingly soluble in water (84, 85). The formation of the 1-butanol-enriched phase occurred as 1-butanol solubility decreased in aqueous ABE solution because the solution became more concentrated, with water removed in the form of ice crystals generated during suspension freeze crystallization.

At room temperature, the prepared feed solutions, 3:8:1:88 and 10:17:2:71 ABEW, were homogenous one-liquid phase solutions. However, the 6:16:2:76 ABEW feed solution consisted of two liquid phases: a water-enriched phase and a 1-butanol-enriched phase. It was determined that the 1-butanol enriched phase comprised 12 % of the 6:16:2:76 ABEW feed solution that consisted of two liquid phases.

The suspension freeze crystallization experiments were performed for certain ranges of undercooling degrees: 0.39 °C – 1.15 °C for 3:8:1:88 ABEW, 0.26 °C – 0.84 °C for 6:16:2:76 ABEW, and 0.35 °C – 0.78 °C for 10:17:2:71 ABEW. The suspension freeze crystallization of the ABE solutions and 1-butanol phase formation and separation from the mother liquor are shown in Figure 21.

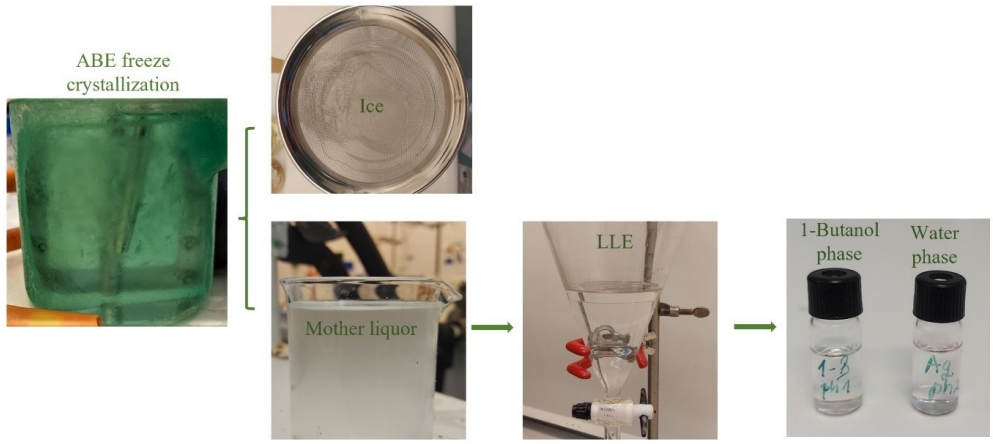

Figure 21. 1-butanol separation from synthetic ABE solutions.

During cooling in the suspension freeze crystallizer prior to ice seeding, it was noticeable that a 1-butanol enriched phase started to form and to increase in quantity in the case of the

10:17:2:71 ABEW and 6:16:2:76 ABEW solutions, respectively (Paper 3). This phenomenon was not observed during the freeze crystallization of 3:8:1:88 ABEW, because a smaller amount of 1-butanol enriched phase was formed, which was on average 2 grams for the applied range of undercooling degrees. However, after freeze crystallization and ice removal, the 1-butanol phase formed from the mother liquor inside the enclosed separatory funnel.
The 1-butanol yield is expressed as the percentage ratio of the masses of separated 1-butanol in the form of a butanol-enriched phase and 1-butanol in the feed ABE solution. It was observed that, as expected, 1-butanol yields increased with the higher undercooling degrees applied for the suspension freeze crystallization experiments because more water in the form of ice crystals was removed (Paper 3). The average yields and purities of 1-butanol separated from 3:8:1:88, 6:16:2:76, and 10:17:2:71 ABEW solutions for the ranges of undercooling degrees applied are given in Figure 22.

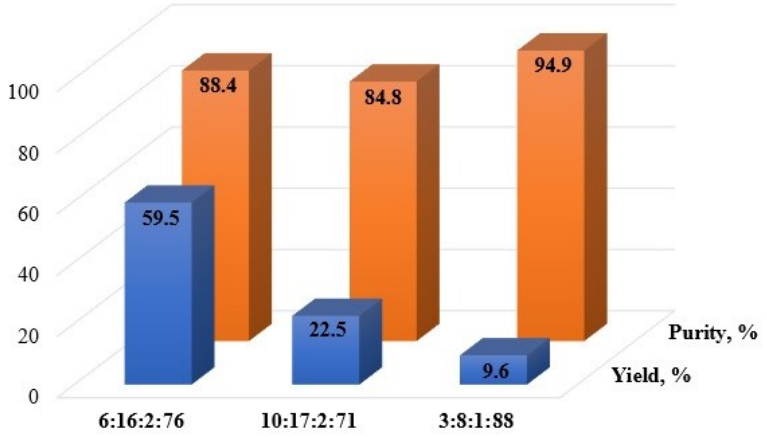

Figure 22. Average 1-butanol yield (mass of 1-butanol in 1-butanol enriched fraction/initial mass of 1-butanol) and 1-butanol content in 1-butanol liquid phase separated from synthetic ABE solutions.

The average 1-butanol yields obtained from different solutions increased in order, from 3:8:1:88 ABEW to 6:16:2:76 ABEW. The reasons for this are the higher initial amount of 1-butanol in the 6:16:2:76 ABEW and 10:17:2:71 ABEW feed solutions in comparison with 3:8:1:88 ABEW, and the lower solubility of 1-butanol in the former solutions in comparison with 3:8:1:88 ABEW. The average purities of separated 1-butanol were in the range of 84.8% to 94.9%. Based on gas chromatography analysis, it was determined that the 1-butanol separated from 3:8:1:88 ABEW, 6:16:2:76 ABEW, and 10:17:2:71 ABEW solutions contained mostly water as an impurity and 0.11 wt.%, 0.27 wt.%, and 0.35 wt.% combined acetone and ethanol impurities, respectively.
After the 1-butanol separation, water-enriched phases were analyzed to determine the concentration of butanol and other solvents remaining in the water phases. The concentration factor was expressed as a ratio of the 1-butanol concentration in the water-enriched phase and 1-butanol in the feed ABE solution. The average concentration factor values for 1-butanol for 3:8:1:88, 6:16:2:76, and 10:17:2:71 ABEW solutions are shown in Figure 23.

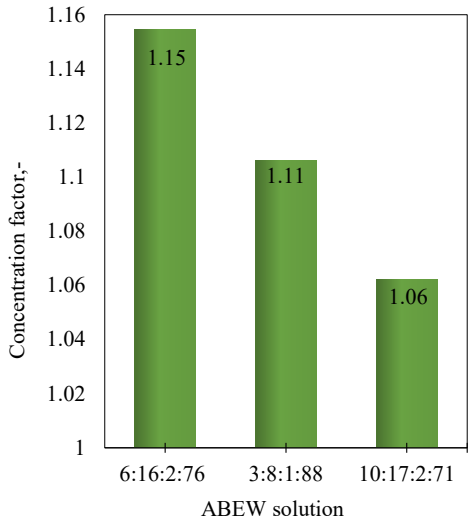

Figure 23. Average 1-butanol concentration factors (mass fraction of 1-butanol in water-enriched fraction / initial mass fraction of 1-butanol) for synthetic ABE solutions.

In Figure 23 it is apparent that 1-butanol was concentrated in the remaining water-enriched phase formed in the two-liquid phase system. However, the acetone present in the water-enriched phase had a lower concentration than in the feed ABE solutions because of its low vapor pressure and loss during the separation of ice crystals and liquid phases after freeze crystallization. On average, the relative loss of acetone varied from 8.4% to 33.3% and to 40.7% for 10:17:2:71 ABEW, 6:16:2:76 ABEW, and 3:8:1:88 ABEW solutions, respectively. In the case of ethanol, no clear conclusion can be made regarding whether it was concentrated or diluted in the water-enriched phase because both phenomena were present, depending on the samples. Therefore, in water-enriched phases separated from 10:17:2:71 ABEW solutions, the ethanol was concentrated with an average concentration factor of 1.35. However, the ethanol loss in water-enriched phase samples was on average 13.7 % and 17.7 % for 3:8:1:88 ABEW and 6:16:2:76 ABEW solutions, respectively.

7. Levoglucosan recovery from pyrolysis oil

Levoglucosan is an anhydrous sugar formed from cellulose during its thermal decomposition. Hence, it is produced via the pyrolysis of cellulosic and lignocellulosic materials (86-89). In nature, it is generated during forest fires (90, 91). Levoglucosan can be applied as a platform molecule for the synthesis of biopolymers and drugs or converted to other high-value chemicals, such as levoglucosenone and glucose, which are further used in drug and fuel production, respectively (92-95).

In this work, levoglucosan was recovered from supersaturated aqueous pyrolysis oil extract solution by cooling crystallization. Levoglucosan solubility in synthetic aqueous solutions and the concentrations of organic acids (formic and acetic), like their concentrations in aqueous pyrolysis extract, were determined at temperatures of 25 °C and 50 °C. The solubility test procedure and experimental procedure for crystallization from solution by cooling are explained in Publication 4.

The levoglucosan solubility in synthetic solutions was 153 g/100 g (solvents) and 203 g/100 g (solvents) at 25 °C and 50 °C, respectively. Levoglucosan solubility in synthetic solutions due to the presence of organic acids was reduced to approx. 67% at a temperature of 50 °C in comparison with levoglucosan solubility in pure water. However, this difference between the above-mentioned solutions was insignificant at 25 °C. The supersaturated solution, prepared by adding commercial levoglucosan to 1:1 pyrolysis oil extract, was fed into a reactor and cooled from 35 °C to 5 °C at two different cooling rates, i.e., 0.5 K/min and 0.8 K/min. Levoglucosan seed crystals of approximately 40 mg were added to the supersaturated PO extract when it reached 30 °C. After 60 minutes of aging time, the levoglucosan crystals were separated from the mother liquor, washed with ethyl acetate, and dried in a vacuum oven. During the washing, it was observed that levoglucosan crystals tend to agglomerate. The average levoglucosan recovery rate, determined as the percentage ratio of the masses of dried recovered levoglucosan and levoglucosan in the supersaturated 1:1 PO extract feed, was 24%. Samples of dried levoglucosan crystals are shown in Figure 24.

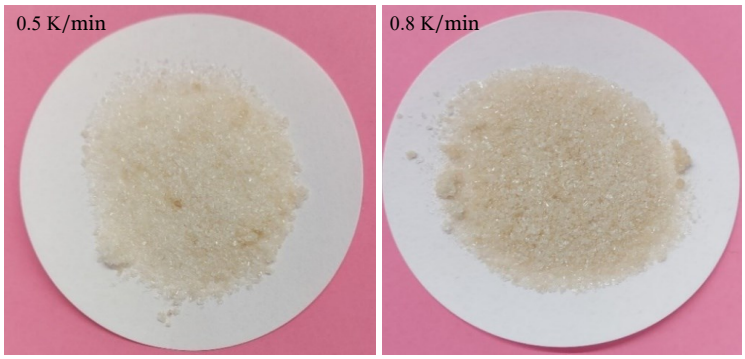

Figure 24. Levoglucosan crystals obtained from supersaturated 1:1 pyrolysis oil extract with cooling rates of 0.5 K/min and 0.8 K/min.

The particle size distributions (PSD) of levoglucosan crystals were measured by Malvern Particle sizer. Shape and morphology of the samples, and the phase transition were investigated by means of SEM, XRD and DSC analyses.
The typical SEM image of levoglucosan sample formed with cooling rate of 0.8 K/m is shown in Figure 25.

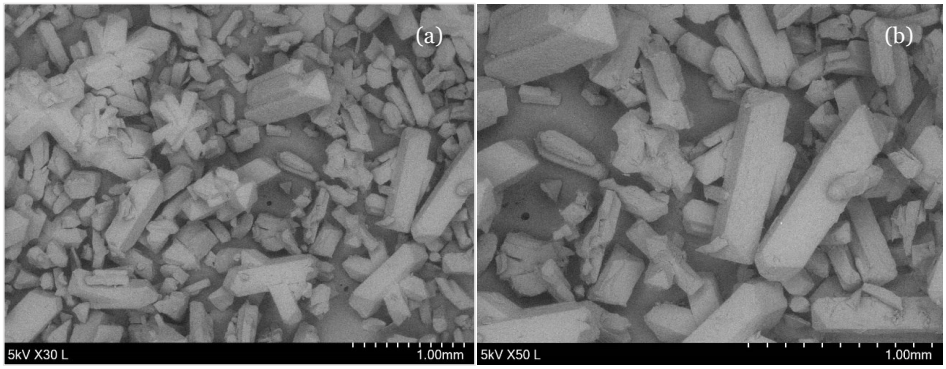

Figure 25. SEM images of levoglucosan crystals produced with cooling rate of 0.8 K/min captured at (a) 30 L and (b) 50 L.

Rod-shaped levoglucosan crystals with an average size of 846.5 μm were recovered from the supersaturated 1:1 PO extract. Agglomeration of smaller particles was detected based on PSD measurements. The sharp and intense crystalline peak appeared at 2θ of 18°. PSD curves and XRD patterns of recovered samples are included in Paper 4. The phase transitions of commercial levoglucosan and levoglucosan recovered with cooling rates of 0.5 K/min and 0.8 K/min are shown on DSC thermograms in Figure 26.

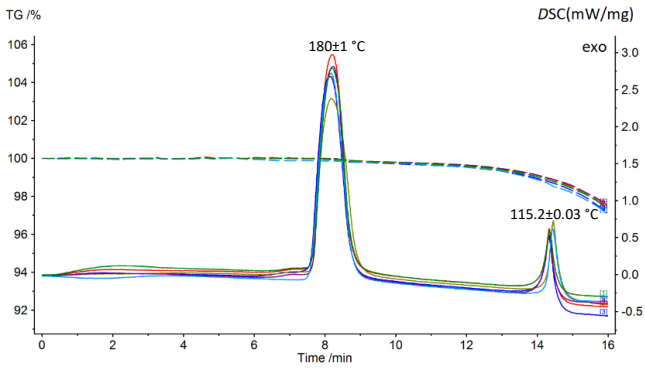

Figure 26. DSC curves of commercial and obtained levoglucosan crystals by cooling rates of 0.5 K/min and 0.8 K/min in batch cooling crystallization experiments.

For levoglucosan samples, two melting peaks were observed upon heating on the DSC thermograms. The first phase transition occurred at 180±1 °C. At this temperature, levoglucosan crystal transitions into unstable form, i.e., plastic crystal, before it melts at 115.2±0.03 °C which corresponds to the second observed melting peak (Paper 4). Similar phase transitions of crystalline levoglucosan have been reported previously by Tombari et al. (98).

8. Summary

The main objective of this doctoral thesis was the development and application of a concentration method based on the freeze crystallization methods of layer and suspension crystallization for aqueous solutions related to the biorefinery field. The motivation was to potentially replace evaporative-based separation methods and henceforth reduce energy consumption by up to seven times in cases when water is removed in the form of ice rather than vapor. Moreover, water removal from multi-component solutions is a necessary step in biorefinery downstream processing. It hinders undesirable chemical reactions between solution compounds, which is typical for pyrolysis oil (etherification, esterification) and ionic liquid solutions (hydrolysis) and facilitates the separation of valuable biochemicals from concentrated solutions in combination with other separation methods. Concentrations of various biorefinery process solutions: ABE fermentation broths, aqueous PO extracts, and [DBNH][OAc], were experimentally investigated using suspension freeze crystallization. Experimental studies on layer freeze crystallization were conducted for aqueous [DBNH][OAc] solutions and aqueous sucrose solutions. In the modeling part, the focus was on a numerical study performed by CFD analysis of heat transfer during the cooling stages of sucrose solutions inside a crystallizer equipped with a cold finger. A summary of the observations and results obtained is given in the following text.

The solid-liquid equilibria of a binary [DBNH][OAc] IL water compound system were investigated by DSC, whereas the freezing points of various aqueous solutions mentioned above were determined by suspension freeze crystallization initiated by ice seeding. Based on the binary [DBNH][OAc] IL-water phase diagram, crystallization could be developed for [DBNH][OAc] IL-water solutions from a water-enriched region. The corresponding freezing points of aqueous 3 wt.% and 6 wt.% [DBNH][OAc] obtained by both DSC and SFC were slightly different because the ice crystallization kinetics for spontaneous ice crystallization (DSC) and seeded ice crystallization (SFC) differ. The obtained freezing points of various aqueous solutions were in the range from -0.56 °C to -7.51 °C. The as-obtained freezing point values were not so much below zero, therefore freeze crystallization is considered to be a feasible concentration method. Aqueous sucrose, ABE solutions, and the modeled PO solution (neglecting minor compounds) were ideal solutions, whereas [DBNH][OAc] was a non-ideal solution based on the activity coefficients of water determined with the Van't Hoff equation. Ice crystallization kinetic investigations were divided into studies on nucleation rate per single crystal and studies on the overall crystal growth rate. The initial amount of water in the solution and applied subcooling degree had a major effect on the nucleation rates. For an

undercooling range of 0.31-1.87 °C, the nucleation rate per single ice crystal increased for aqueous solutions in the following order: PO extract solutions, ABE solutions, and [DBNH][OAc] solutions. Even though the [DBNH][OAc] solution was non-ideal with attractive intermolecular forces, it had the fastest ice nucleation kinetics because the initial water content and undercooling degrees applied were the highest. The overall mass crystal growth rates for different solutions studied with suspension freeze crystallization at an undercooling range of 0.26-1.89 °C had a magnitude of order between 10-5 and 10-3. For the same type of feed solution (either ABE, PO, [DBNH][OAc]) but with different concentrations, the growth rate depended on the initial amount of water. For different types of solutions, it was observed that solution ideality noticeably affected the ice growth kinetics in relation to suspension freeze crystallization. The ice growth for an ideal 3:8:1:88 ABEW solution proceeded with faster trends in comparison with the ice growth for non-ideal [DBNH][OAc] solutions, even though the undercooling and water amounts were higher in the latter case. Undercooling had the biggest impact on the ice growth kinetics of PO extracts, e.g., overall ice growth rates for the 1:5 PO extract significantly increased when undercooling was higher. The overall growth rates of ice layers formed from [DBNH][OAc] and sucrose solutions were 10-4 and 10-3 for an undercooling range of 0.76 - 2.35 °C, respectively. The overall growth rates of ice layers were clearly dependent on the solution ideality and initial water concentration. Therefore, the ice layers for ideal and more concentrated sucrose solutions formed with slightly slower kinetics than for non-ideal, more dilute [DBNH][OAc] solutions.

Based on the determined ice yield and distribution coefficient, the SFC method could be considered to be an efficient concentration method. The ice yield (which in general increased for higher undercooling degrees) obtained with SFC for 60 minutes of freezing has a maximum value of 68% (undercooling degree 1.26 °C) for the 1:5 PO extract and 35.6% (1.87 °C) for the [DBNH][OAc] solution. Even though the PO extract solutions were less concentrated and the undercooling degree was lower, they had higher yields than [DBNH][OAc]. The model PO extract was an ideal solution, but the interactions of all components in such a complex system as PO extract may explain this phenomenon. Ice yields obtained for 80 minutes of freezing from ABE fermentation broths and synthetic ABE solutions (3:8:1:88 ABEW, 10:17:2:71 ABEW) increased because of the higher initial water amount. Therefore, a maximum yield of 86.7% (undercooling degree of 1.07 °C) for ABE fermentation broth, and 21.5% (for an undercooling degree of 0.78 °C) was achieved. The washed ice crystals were pure with a distribution coefficient value of 0 for the ABE fermentation broths, ABE solutions, and PO extracts and very pure (0.26) for the [DBNH][OAc] solutions. Yields obtained with layer freeze crystallization for 60 minutes of freezing were up to 7.15% and 5.8% for the [DBNH][OAc] and sucrose solutions, respectively. The average distribution coefficients were up to 0.38 and 0.62 for the above-mentioned solutions. Ice yields and related purities to produce ice crystals with LFC were lower than with SFC. First, the yields were lower because of the much smaller cooling surface area available for LFC. The purities were lower because solute molecules were trapped between the ice grains.

The influence on the thermophysical properties of the solutions on the cooling stage inside the crystallizer with a cold finger was investigated by CFD for model 10 wt.%, 23 wt.%, and 30 wt.% sucrose solutions. Based on the obtained temperature distribution and convective heat transfer coefficients, undercooling was achieved fastest for the 10 wt.%, followed by 23 wt. %, and 30 wt.% solutions.

1-butanol was separated from the synthetic ABE solutions due to its reduced solubility when water is removed by suspension freezing crystallization. Average cumulative yields of separated 1-butanol were 9.6%, (for 3:8:1:88 ABEW), 22.5% (for 10:17:2:71 ABEW), and 59.5% (for 6:16.2:76 ABEW) with purities in the range from 84.8% to 94.9%. Levoglucosan crystals, obtained by cooling crystallization from supersaturated 1:5 PO extract solutions were rod-shaped with a tendency to agglomerate during washing.

Some considerations for future studies are discussed below:

- Freeze crystallization studies could be considered as a potential concentration method for aqueous [DBNH][OAc] solutions taken from industrial stream.
- It was noticed that freeze crystallization for ABE solutions occurs spontaneously, and a lower range of undercooling degrees was applied than for other solutions to prevent this phenomenon. More comprehensive studies on the metastability zone could be conducted to obtain an even better understanding of the nucleation kinetics of various solutions.
- LFC is usually applied for viscous solutions, so a CFD heat transfer study could be integrated with a mass transfer study and simulation of ice crystallization.
- Biorefinery process solutions, ABE fermentation broths, and PO extracts with a higher initial concentration of target biochemicals could be tested. Otherwise, FC should be integrated with other separation technologies as a pre- or post- step method in order to separate target biochemicals. One possible option could be to integrate FC with antisolvent crystallization. Appropriate selection of antisolvents would reduce levoglucosan solubility.

References

(1) Demand for Manufacturing: Driving Inclusive and Sustainable Industrial Development; UNIDO, Ed.; Industrial development report; UNIDO: Vienna, 2017.

(2) Industry; IEA: Paris, 2022. https://www.iea.org/reports/industry, License: CC BY 4.0

(3) Kiss, A. A.; Smith, R. Rethinking Energy Use in Distillation Processes for a More Sustainable Chemical Industry. Energy 2020, 203, 117788. https://doi.org/10.1016/j.energy.2020.117788.

(4) Seader, J. D.; Henley, E. J. Separation Process Principles; Wiley: New York, 1998.

(5) Staff, N. A. P. Separation Technologies for the Industries of the Future; National Academies Press: Washington, 1998.

(6) Coulson, J. M.; Richardson, J. F. Chemical Engineering. 2: Particle Technology and Separation Processes, 5. ed., repr.; Butterworth Heinemann: Amsterdam, 2010.

(7) The Role of Bioenergy in the Emerging Bioeconomy: Resources, Technologies, Sustainability and Policy; Lago, C., Caldés, N., Lechón, Y., Eds.; Academic Press: Amsterdam, 2018.

(8) Mohan, D.; Pittman, C. U.; Steele, P. H. Pyrolysis of Wood/Biomass for Bio-Oil: A Critical Review. Energy Fuels 2006, 20 (3), 848–889. https://doi.org/10.1021/ef0502397.

(9) Bergeron, C. Biorefinery Co-Products: Phytochemicals, Primary Metabolites and Value-Added Biomass Processing; Biorefinery co-products; John Wiley & Sons: Chichester, West Sussex Hoboken, 2012.

(10) Aslanzadeh, S.; Ishola, M. M.; Richards, T.; Taherzadeh, M. J. An Overview of Existing Individual Unit Operations. In Biorefineries; Elsevier, 2014; pp 3–36. https://doi.org/10.1016/B978-0-444-59498-3.00001-4.

(11) Gollakota, A. R. K.; Reddy, M.; Subramanyam, M. D.; Kishore, N. A Review on the Upgradation Techniques of Pyrolysis Oil. Renewable and Sustainable Energy Reviews 2016, 58, 1543–1568. https://doi.org/10.1016/j.rser.2015.12.180.

(12) Bhatnagar, A.; Tolvanen, H.; Konttinen, J. Potential of Stepwise Pyrolysis for On-Site Treatment of Agro-Residues and Enrichment of Value-Added Chemicals. Waste Management 2020, 118, 667–676. https://doi.org/10.1016/j.wasman.2020.09.022.

(13) Mukarakate, C.; Evans, R. J.; Deutch, S.; Evans, T.; Starace, A. K.; ten Dam, J.; Watson, M. J.; Magrini, K. Reforming Biomass Derived Pyrolysis Bio-Oil Aqueous Phase to Fuels. Energy Fuels 2017, 31 (2), 1600–1607. https://doi.org/10.1021/acs.energyfuels.6b02463.

(14) Alam, Md. S.; Tanveer, Md. S. Conversion of Biomass into Biofuel: A Cutting-Edge Technology. In Bioreactors; Elsevier, 2020; pp 55–74. https://doi.org/10.1016/B978-0-12-821264-6.00005-X.

(15) Veza, I.; Muhamad Said, M. F.; Latiff, Z. A. Recent Advances in Butanol Production by Acetone-Butanol-Ethanol (ABE) Fermentation. Biomass and Bioenergy 2021, 144, 105919. https://doi.org/10.1016/j.biombioe.2020.105919.

(16) Chandgude, V.; Välisalmi, T.; Linnekoski, J.; Granström, T.; Pratto, B.; Eerikäinen, T.; Jurgens, G.; Bankar, S. Reducing Agents Assisted Fed-Batch Fermentation to Enhance ABE Yields. Energy Conversion and Management 2021, 227, 113627. https://doi.org/10.1016/j.enconman.2020.113627.
(17) Pratto, B.; Chandgude, V.; de Sousa, R.; Cruz, A. J. G.; Bankar, S. Biobutanol Production from Sugarcane Straw: Defining Optimal Biomass Loading for Improved ABE Fermentation. Industrial Crops and Products 2020, 148, 112265. https://doi.org/10.1016/j.indcrop.2020.112265.
(18) Stepan, A. M.; Michud, A.; Hellstén, S.; Hummel, M.; Sixta, H. IONCELL-P&F: Pulp Fractionation and Fiber Spinning with Ionic Liquids. Ind. Eng. Chem. Res. 2016, 55 (29), 8225–8233. https://doi.org/10.1021/acs.iecr.6b00071.
(19) Elsayed, S.; Hummel, M.; Sawada, D.; Guizani, C.; Rissanen, M.; Sixta, H. Superbase-Based Protic Ionic Liquids for Cellulose Filament Spinning. Cellulose 2021, 28 (1), 533–547. https://doi.org/10.1007/s10570-020-03505-y.
(20) Nypelö, T.; Asaadi, S.; Kneidinger, G.; Sixta, H.; Konnerth, J. Conversion of Wood-Biopolymers into Macrofibers with Tunable Surface Energy via Dry-Jet Wet-Spinning. Cellulose 2018, 25 (9), 5297–5307. https://doi.org/10.1007/s10570-018-1902-4.
(21) Michud, A.; Tanttu, M.; Asaadi, S.; Ma, Y.; Netti, E.; Kääriainen, P.; Persson, A.; Berntsson, A.; Hummel, M.; Sixta, H. Ioncell-F: Ionic Liquid-Based Cellulosic Textile Fibers as an Alternative to Viscose and Lyocell. Textile Research Journal 2016, 86 (5), 543–552. https://doi.org/10.1177/0040517515591774.
(22) Ramaswamy, S. Separation and Purification Technologies in Biorefineries; John Wiley & Sons Inc: Chichester, West Sussex, United Kingdom, 2013.
(23) Lê, H. Q.; Sixta, H.; Hummel, M. Ionic Liquids and Gamma-Valerolactone as Case Studies for Green Solvents in the Deconstruction and Refining of Biomass. Current Opinion in Green and Sustainable Chemistry 2019, 18, 20–24. https://doi.org/10.1016/j.cogsc.2018.11.009.
(24) Cho, C.-W.; Song, M.-H.; Pham, T. P. T.; Yun, Y.-S. Environmental Concerns Regarding Ionic Liquids in Biotechnological Applications. In Application of Ionic Liquids in Biotechnology; Itoh, T., Koo, Y.-M., Eds.; Advances in Biochemical Engineering/Biotechnology; Springer International Publishing: Cham, 2018; Vol. 168, pp 241–328. https://doi.org/10.1007/10_2018_79.
(25) Mai, N. L.; Ahn, K.; Koo, Y.-M. Methods for Recovery of Ionic Liquids—A Review. Process Biochemistry 2014, 49 (5), 872–881. https://doi.org/10.1016/j.procbio.2014.01.016.
(26) Kuzmina, O. Methods of IL Recovery and Destruction. In Application, Purification, and Recovery of Ionic Liquids; Elsevier, 2016; pp 205–248. https://doi.org/10.1016/B978-0-444-63713-0.00005-5.
(27) Zhou, J.; Sui, H.; Jia, Z.; Yang, Z.; He, L.; Li, X. Recovery and Purification of Ionic Liquids from Solutions: A Review. RSC Adv. 2018, 8 (57), 32832–32864. https://doi.org/10.1039/C8RA06384B.
(28) Huang, H.-J.; Ramaswamy, S.; Liu, Y. Separation and Purification of Biobutanol during Bioconversion of Biomass. Separation and Purification Technology 2014, 132, 513–540. https://doi.org/10.1016/j.seppur.2014.06.013.
(29) Pinheiro Pires, A. P.; Arauzo, J.; Fonts, I.; Domine, M. E.; Fernández Arroyo, A.; Garcia-Perez, M. E.; Montoya, J.; Chejne, F.; Pfromm, P.; Garcia-Perez, M. Challenges and Opportunities for Bio-Oil Refining: A Review. Energy Fuels 2019, 33 (6), 4683–4720. https://doi.org/10.1021/acs.energyfuels.9b00039.

(30) Drugkar, K.; Rathod, W.; Sharma, T.; Sharma, A.; Joshi, J.; Pareek, V. K.; Ledwani, L.; Diwekar, U. Advanced Separation Strategies for Up-Gradation of Bio-Oil into Value-Added Chemicals: A Comprehensive Review. Separation and Purification Technology 2022, 283, 120149. https://doi.org/10.1016/j.seppur.2021.120149.
(31) Chan, Y. H.; Loh, S. K.; Chin, B. L. F.; Yiin, C. L.; How, B. S.; Cheah, K. W.; Wong, M. K.; Loy, A. C. M.; Gwee, Y. L.; Lo, S. L. Y.; Yusup, S.; Lam, S. S. Fractionation and Extraction of Bio-Oil for Production of Greener Fuel and Value-Added Chemicals: Recent Advances and Future Prospects. Chemical Engineering Journal 2020, 397, 125406. https://doi.org/10.1016/j.cej.2020.125406.
(32) Kiss, A. A.; Lange, J.-P.; Schuur, B.; Brilman, D. W. F.; van der Ham, A. G. J.; Kersten, S. R. A. Separation Technology–Making a Difference in Biorefineries. Biomass and Bioenergy 2016, 95, 296–309. https://doi.org/10.1016/j.biombioe.2016.05.021.
(33) Qi, X.; Li, L.; Tan, T.; Chen, W.; Smith, R. L. Adsorption of 1-Butyl-3-Methylimidazolium Chloride Ionic Liquid by Functional Carbon Microspheres from Hydrothermal Carbonization of Cellulose. Environ. Sci. Technol. 2013, 47 (6), 2792–2798. https://doi.org/10.1021/es304873t.
(34) Qi, X.; Li, L.; Wang, Y.; Liu, N.; Smith, R. L. Removal of Hydrophilic Ionic Liquids from Aqueous Solutions by Adsorption onto High Surface Area Oxygenated Carbonaceous Material. Chemical Engineering Journal 2014, 256, 407–414. https://doi.org/10.1016/j.cej.2014.07.020.
(35) Wang, Y.; Bai, C.; Yan, L.; Qi, X. Adsorption of Imidazolium-Based Ionic Liquids from Aqueous Solution onto Cellulose-Derived Activated Carbon Materials. Journal of Environmental Chemical Engineering 2015, 3 (4), 2426–2434. https://doi.org/10.1016/j.jece.2015.09.016.
(36) Lemus, J.; Moya, C.; Gilarranz, M. A.; Rodriguez, J. J.; Palomar, J. Fixed-Bed Adsorption of Ionic Liquids onto Activated Carbon from Aqueous Phase. Journal of Environmental Chemical Engineering 2017, 5 (6), 5347–5351. https://doi.org/10.1016/j.jece.2017.10.014.
(37) Stanford, J. P.; Hall, P. H.; Rover, M. R.; Smith, R. G.; Brown, R. C. Separation of Sugars and Phenolics from the Heavy Fraction of Bio-Oil Using Polymeric Resin Adsorbents. Separation and Purification Technology 2018, 194, 170–180. https://doi.org/10.1016/j.seppur.2017.11.040.
(38) Raganati, F.; Procentese, A.; Olivieri, G.; Russo, M. E.; Salatino, P.; Marzocchella, A. Bio-Butanol Recovery by Adsorption/Desorption Processes. Separation and Purification Technology 2020, 235, 116145. https://doi.org/10.1016/j.seppur.2019.116145.
(39) Huang, K.; Wu, R.; Cao, Y.; Li, H.; Wang, J. Recycling and Reuse of Ionic Liquid in Homogeneous Cellulose Acetylation. Chinese Journal of Chemical Engineering 2013, 21 (5), 577–584. https://doi.org/10.1016/S1004-9541(13)60524-8.
(40) Wang, Y.; Wang, S.; Leng, F.; Chen, J.; Zhu, L.; Luo, Z. Separation and Characterization of Pyrolytic Lignins from the Heavy Fraction of Bio-Oil by Molecular Distillation. Separation and Purification Technology 2015, 152, 123–132. https://doi.org/10.1016/j.seppur.2015.08.011.
(41) Wang, S.; Gu, Y.; Liu, Q.; Yao, Y.; Guo, Z.; Luo, Z.; Cen, K. Separation of Bio-Oil by Molecular Distillation. Fuel Processing Technology 2009, 90 (5), 738–745. https://doi.org/10.1016/j.fuproc.2009.02.005.
(42) Weerachanchai, P.; Lee, J.-M. Recyclability of an Ionic Liquid for Biomass Pretreatment. Bioresource Technology 2014, 169, 336–343. https://doi.org/10.1016/j.biortech.2014.06.072.
(43) Nam, H.; Choi, J.; Capareda, S. C. Comparative Study of Vacuum and Fractional Distillation Using Pyrolytic Microalgae (Nannochloropsis Oculata) Bio-Oil. Algal Research 2016, 17, 87–96. https://doi.org/10.1016/j.algal.2016.04.020.

(44) Grisales Diaz, V. H.; Olivar Tost, G. Energy Efficiency of Acetone, Butanol, and Ethanol (ABE) Recovery by Heat-Integrated Distillation. Bioprocess Biosyst Eng 2018, 41 (3), 395–405. https://doi.org/10.1007/s00449-017-1874-z.
(45) Lynam, J. G.; Chow, G. I.; Coronella, C. J.; Hiibel, S. R. Ionic Liquid and Water Separation by Membrane Distillation. Chemical Engineering Journal 2016, 288, 557–561. https://doi.org/10.1016/j.cej.2015.12.028.34.
(46) Wu, H.; Shen, F.; Wang, J.; Luo, J.; Liu, L.; Khan, R.; Wan, Y. Separation and Concentration of Ionic Liquid Aqueous Solution by Vacuum Membrane Distillation. Journal of Membrane Science 2016, 518, 216–228. https://doi.org/10.1016/j.memsci.2016.07.017.
(47) Wang, Y.; Qiu, B.; Fan, S.; Liu, J.; Qin, Y.; Jian, S.; Wang, Y.; Xiao, Z. Membrane Distillation of Butanol from Aqueous Solution with Polytetrafluoroethylene Membrane. Chem. Eng. Technol. 2020, 43 (6), 1160–1166. https://doi.org/10.1002/ceat.201900484.
(48) Gupta, O.; Roy, S.; Mitra, S. Low Temperature Recovery of Acetone–Butanol–Ethanol (ABE) Fermentation Products via Microwave Induced Membrane Distillation on Carbon Nanotube Immobilized Membranes. Sustainable Energy Fuels 2020, 4 (7), 3487–3499. https://doi.org/10.1039/D0SE00461H.
(49) Sun, J.; Shi, J.; Murthy Konda, N. V. S. N.; Campos, D.; Liu, D.; Nemser, S.; Shamshina, J.; Dutta, T.; Berton, P.; Gurau, G.; Rogers, R. D.; Simmons, B. A.; Singh, S. Efficient Dehydration and Recovery of Ionic Liquid after Lignocellulosic Processing Using Pervaporation. Biotechnol Biofuels 2017, 10 (1), 154. https://doi.org/10.1186/s13068-017-0842-9.
(50) Li, S.-Y.; Srivastava, R.; Parnas, R. S. Study of in Situ 1-Butanol Pervaporation from A-B-E Fermentation Using a PDMS Composite Membrane: Validity of Solution-Diffusion Model for Pervaporative A-B-E Fermentation. Biotechnol Progress 2011, 27 (1), 111–120. https://doi.org/10.1002/btpr.535.
(51) Chen, H.; Cai, D.; Chen, C.; Wang, J.; Qin, P.; Tan, T. Novel Distillation Process for Effective and Stable Separation of High-Concentration Acetone–Butanol–Ethanol Mixture from Fermentation–Pervaporation Integration Process. Biotechnol Biofuels 2018, 11 (1), 286. https://doi.org/10.1186/s13068-018-1284-8.
(52) Cheng, C.; Liu, F.; Yang, H. K.; Xiao, K.; Xue, C.; Yang, S.-T. High-Performance n -Butanol Recovery from Aqueous Solution by Pervaporation with a PDMS Mixed Matrix Membrane Filled with Zeolite. Ind. Eng. Chem. Res. 2020, 59 (16), 7777–7786. https://doi.org/10.1021/acs.iecr.9b06104.
(53) F. Fernández, J. Recovery of Ionic Liquids from Wastewater by Nanofiltration. J Membra Sci Technol 2013, 03 (03). https://doi.org/10.4172/2155-9589.S4-001.
(54) Endo, T.; Tatsumi, M.; Kuroda, K.; Satria, H.; Shimada, Y.; Ninomiya, K.; Takahashi, K. Efficient Recovery of Ionic Liquid by Electrodialysis in the Acid Hydrolysis Process. Separation Science and Technology 2017, 52 (7), 1240–1245. https://doi.org/10.1080/01496395.2017.1281957.
(55) Teella, A.; Huber, G. W.; Ford, D. M. Separation of Acetic Acid from the Aqueous Fraction of Fast Pyrolysis Bio-Oils Using Nanofiltration and Reverse Osmosis Membranes. Journal of Membrane Science 2011, 378 (1–2), 495–502. https://doi.org/10.1016/j.memsci.2011.05.036.
(56) Holding, A. J.; Parviainen, A.; Kilpeläinen, I.; Soto, A.; King, A. W. T.; Rodríguez, H. Efficiency of Hydrophobic Phosphonium Ionic Liquids and DMSO as Recyclable Cellulose Dissolution and Regeneration Media. RSC Adv. 2017, 7 (28), 17451–17461. https://doi.org/10.1039/C7RA01662J.

(57) del Pozo, C.; Bartrolí, J.; Puy, N.; Fàbregas, E. Separation of Value-Added Chemical Groups from Bio-Oil of Olive Mill Waste. Industrial Crops and Products 2018, 125, 160–167. https://doi.org/10.1016/j.indcrop.2018.08.062.
(58) Yu, H.; Cui, K.; Li, T.; Zhang, Z.; Zhou, Z.; Ren, Z. Recovery of Butanol from ABE Fermentation Broth with Hydrophobic Functionalized Ionic Liquids as Extractants. ACS Sustainable Chem. Eng. 2019, 7 (10), 9318–9329. https://doi.org/10.1021/acssuschemeng.9b00434.
(59) Plaza, P. E.; Coca, M.; Yagüe, S. L.; Gutiérrez, G.; Rochón, E.; García-Cubero, M. T. Bioprocess Intensification for Acetone-Butanol-Ethanol Fermentation from Brewer's Spent Grain: Fed-Batch Strategies Coupled with in-Situ Gas Stripping. Biomass and Bioenergy 2022, 156, 106327. https://doi.org/10.1016/j.biombioe.2021.106327.
(60) Kongjan, P.; Tohlang, N.; Khaonuan, S.; Cheirsilp, B.; Jariyaboon, R. Characterization of the Integrated Gas Stripping-Condensation Process for Organic Solvent Removal from Model Acetone-Butanol-Ethanol Aqueous Solution. Biochemical Engineering Journal 2022, 182, 108437. https://doi.org/10.1016/j.bej.2022.108437.
(61) Lodi, G.; De Guido, G.; Pellegrini, L. A. Simulation and Energy Analysis of the ABE Fermentation Integrated with Gas Stripping. Biomass and Bioenergy 2018, 116, 227–235. https://doi.org/10.1016/j.biombioe.2018.06.012.
(62) Yang, S.-T. Bioprocessing for Value-Added Products from Renewable Resources: New Technologies and Applications; Elsevier Science: Burlington, 2011.
(63) Oudshoorn, A.; van der Wielen, L. A. M.; Straathof, A. J. J. Assessment of Options for Selective 1-Butanol Recovery from Aqueous Solution. Ind. Eng. Chem. Res. 2009, 48 (15), 7325–7336. https://doi.org/10.1021/ie900537w.
(64) Liu, Y.; Meyer, A. S.; Nie, Y.; Zhang, S.; Thomsen, K. Low Energy Recycling of Ionic Liquids via Freeze Crystallization during Cellulose Spinning. Green Chem. 2018, 20 (2), 493–501. https://doi.org/10.1039/C7GC02880F.
(65) Yuan, W.; Zhang, L.; Chang, Y.; Ma, H.; Fu, P.; Wang, H.; Li, J. Treatment of Biofuel Production Wastewater by a Combined Freezing Method for Resources Recovery and Waste Reduction. Science of The Total Environment 2021, 774, 145173. https://doi.org/10.1016/j.scitotenv.2021.145173.
(66) Dette, S.; Maetz, L. TWICE™ — an ice-cold process for highest food concentration; Sulzer Technical Review Issue 1; Sulzer Chemtech: Winterthur, 2020.
(67) Sánchez, J.; Hernández, E.; Auleda, J. M.; Raventós, M. Freeze Concentration of Whey in a Falling-Film Based Pilot Plant: Process and Characterization. Journal of Food Engineering 2011, 103 (2), 147–155. https://doi.org/10.1016/j.jfoodeng.2010.10.009.
(68) Moreno, F. L.; Raventós, M.; Hernández, E.; Ruiz, Y. Behaviour of Falling-Film Freeze Concentration of Coffee Extract. Journal of Food Engineering 2014, 141, 20–26. https://doi.org/10.1016/j.jfoodeng.2014.05.012.
(69) Lewis, A.; Seckler, M.; Kramer, H.; van Rosmalen, G. Melt Crystallization. In Industrial Crystallization: Fundamentals and Applications; Cambridge University Press: Cambridge, 2015; pp 261–283.
(70) IceCon® Freeze Concentration: Continuous freeze concentration systems; GEA Netherlands, Ed.; GEA Niro PT B.V.: 's-Hertogenbosch, 2022.
(71) Hernández, E.; Raventós, M.; Auleda, J. M.; Ibarz, A. Concentration of Apple and Pear Juices in a Multi-Plate Freeze Concentrator. Innovative Food Science & Emerging Technologies 2009, 10 (3), 348–355. https://doi.org/10.1016/j.ifset.2009.02.001.

(72) Uald Lamkaddam, I.; Vega, E.; Colón, J.; Ponsá, S.; Llenas, L.; Mora, M. Progressive Freeze Concentration of Cheese Whey for Protein and Lactose Recovery. International Dairy Journal 2023, 139, 105572. https://doi.org/10.1016/j.idairyj.2022.105572.
(73) Orellana-Palma, P.; Guerra-Valle, M.; Gianelli, M. P.; Petzold, G. Evaluation of Freeze Crystallization on Pomegranate Juice Quality in Comparison with Conventional Thermal Processing. Food Bioscience 2021, 41, 101106. https://doi.org/10.1016/j.fbio.2021.101106.
(74) Meneses, D. L.; Ruiz, Y.; Hernandez, E.; Moreno, F. L. Multi-Stage Block Freeze-Concentration of Green Tea (Camellia Sinensis) Extract. Journal of Food Engineering 2021, 293, 110381. https://doi.org/10.1016/j.jfoodeng.2020.110381.
(75) Lewis, A. E.; Nathoo, J.; Thomsen, K.; Kramer, H. J.; Witkamp, G. J.; Reddy, S. T.; Randall, D. G. Design of a Eutectic Freeze Crystallization Process for Multicomponent Waste Water Stream. Chemical Engineering Research and Design 2010, 88 (9), 1290–1296. https://doi.org/10.1016/j.cherd.2010.01.023.
(76) Aspeling, B. J.; Chivavava, J.; Lewis, A. E. Selective Salt Crystallization from a Seeded Ternary Eutectic System in Eutectic Freeze Crystallization. Separation and Purification Technology 2020, 248, 117019. https://doi.org/10.1016/j.seppur.2020.117019.
(77) John, M.; Häkkinen, A.; Louhi-Kultanen, M. Purification Efficiency of Natural Freeze Crystallization for Urban Wastewaters. Cold Regions Science and Technology 2020, 170, 102953. https://doi.org/10.1016/j.coldregions.2019.102953.
(78) Tongshuai, L.; Yan, Z.; Yuanqing, T.; Xiaozhuang, W.; Chen, Z.; Nan, W.; Yucan, L. Application of Progressive Freeze Concentration in the Removal of Ca2+ from Wastewater. Journal of Water Process Engineering 2022, 46, 102619. https://doi.org/10.1016/j.jwpe.2022.102619.
(79) Yang, Y.; Lu, Y.; Guo, J.; Zhang, X. Application of Freeze Concentration for Fluoride Removal from Water Solution. Journal of Water Process Engineering 2017, 19, 260–266. https://doi.org/10.1016/j.jwpe.2017.05.009.
(80) Rich, A.; Mandri, Y.; Bendaoud, N.; Mangin, D.; Abderafi, S.; Bebon, C.; Semlali, N.; Klein, J.-P.; Bounahmidi, T.; Bouhaouss, A.; Veesler, S. Freezing Desalination of Sea Water in a Static Layer Crystallizer. Desalination and Water Treatment 2010, 13 (1–3), 120–127. https://doi.org/10.5004/dwt.2010.983.
(81) Zambrano, A.; Ruiz, Y.; Hernández, E.; Raventós, M.; Moreno, F. L. Freeze Desalination by the Integration of Falling Film and Block Freeze-Concentration Techniques. Desalination 2018, 436, 56–62. https://doi.org/10.1016/j.desal.2018.02.015.
(82) Kiwan, S.; Alali, A.; Al-Safadi, M. A Novel Water Freezing Desalination Plant Integrated into a Combined Gas Power Cycle Plant. Energy 2023, 263, 125983. https://doi.org/10.1016/j.energy.2022.125983.
(83) Gmehling, J.; Kolbe, B.; Kleiber, M.; Rarey, J. Chemical Thermodynamics for Process. Simulation; Wiley-VCH Verlag & Co. KGaA: Weinheim, Germany, 2012; pp. 405–437.
(84) Shirai, Y.; Nakanishi, K.; Matsuno, R.; Kamikubo, T. On the Kinetics of Ice Crystallization in Batch Crystallizers. AIChE J. 1985, 31 (4), 676–682. https://doi.org/10.1002/aic.690310418.
(85) John, M.; Suominen, M.; Kurvinen, E.; Hasan, M.; Sormunen, O.-V.; Kujala, P.; Mikkola, A.; Louhi-Kultanen, M. Separation Efficiency and Ice Strength Properties in Simulated Natural Freezing of Aqueous Solutions. Cold Regions Science and Technology 2019, 158, 18–29. https://doi.org/10.1016/j.coldregions.2018.11.006.
(86) Lohmann, J.; Joh, R.; Gmehling, J. Solid–Liquid Equilibria of Viscous Binary Mixtures with Alcohols. J. Chem. Eng. Data 1997, 42 (6), 1170–1175. https://doi.org/10.1021/je9700683.

(87) Okamoto, B. Y.; Wood, R. H.; Thompson, P. T. Freezing Points of Aqueous Alcohols. Free Energy of Interaction of the CHOH, CH2, CONH and C=C Functional Groups in Dilute Aqueous Solutions. J. Chem. Soc., Faraday Trans. 1 1978, 74 (0), 1990. https://doi.org/10.1039/f19787401990.
(88) Osatiashtiani, A.; Zhang, J.; Stefanidis, S. D.; Zhang, X.; Bridgwater, A. V. The Mechanism for Catalytic Fast Pyrolysis of Levoglucosan, Furfural and Furan over HZSM-5: An Experimental and Theoretical Investigation. Fuel 2022, 328, 125279. https://doi.org/10.1016/j.fuel.2022.125279.
(89) Zarei, A.; Zhou, Q.; Yu, H.; Zhang, L. Synergetic Effect of Steam and Activated Tyre Char on the Selective Production of Levoglucosan-Rich Bio-Oil from Catalytic Pyrolysis of Wood Chips. Fuel 2023, 337, 126865. https://doi.org/10.1016/j.fuel.2022.126865.
(90) Bhar, R.; Tiwari, B. R.; Sarmah, A. K.; Brar, S. K.; Dubey, B. K. A Comparative Life Cycle Assessment of Different Pyrolysis-Pretreatment Pathways of Wood Biomass for Levoglucosan Production. Bioresource Technology 2022, 356, 127305. https://doi.org/10.1016/j.biortech.2022.127305.
(91) Li, Q.; Steele, P. H.; Yu, F.; Mitchell, B.; Hassan, E.-B. M. Pyrolytic Spray Increases Levoglucosan Production during Fast Pyrolysis. Journal of Analytical and Applied Pyrolysis 2013, 100, 33–40. https://doi.org/10.1016/j.jaap.2012.11.013.
(92) Hong, Y.; Cao, F.; Fan, M.-Y.; Lin, Y.-C.; Gul, C.; Yu, M.; Wu, X.; Zhai, X.; Zhang, Y.-L. Impacts of Chemical Degradation of Levoglucosan on Quantifying Biomass Burning Contribution to Carbonaceous Aerosols: A Case Study in Northeast China. Science of The Total Environment 2022, 819, 152007. https://doi.org/10.1016/j.scitotenv.2021.152007.
(93) Giannoni, M.; Martellini, T.; Del Bubba, M.; Gambaro, A.; Zangrando, R.; Chiari, M.; Lepri, L.; Cincinelli, A. The Use of Levoglucosan for Tracing Biomass Burning in PM2.5 Samples in Tuscany (Italy). Environmental Pollution 2012, 167, 7–15. https://doi.org/10.1016/j.envpol.2012.03.016.
(94) Longley, C. J.; Fung, D. P. C. Potential Applications and Markets for Biomass-Derived Levoglucosan. In Advances in Thermochemical Biomass Conversion; Bridgwater, A. V., Ed.; Springer Netherlands: Dordrecht, 1993; pp 1484–1494. https://doi.org/10.1007/978-94-011-1336-6_120.
(95) Chen, L.; Zhao, J.; Pradhan, S.; Brinson, B. E.; Scuseria, G. E.; Zhang, Z. C.; Wong, M. S. Ring-Locking Enables Selective Anhydrosugar Synthesis from Carbohydrate Pyrolysis. Green Chem. 2016, 18 (20), 5438–5447. https://doi.org/10.1039/C6GC01600F.
(96) de Souza, P. M.; de Sousa, L. A.; Noronha, F. B.; Wojcieszak, R. Dehydration of Levoglucosan to Levoglucosenone over Solid Acid Catalysts. Tuning the Product Distribution by Changing the Acid Properties of the Catalysts. Molecular Catalysis 2022, 529, 112564. https://doi.org/10.1016/j.mcat.2022.112564.
(97) Linger, J. G.; Hobdey, S. E.; Franden, M. A.; Fulk, E. M.; Beckham, G. T. Conversion of Levoglucosan and Cellobiosan by Pseudomonas Putida KT2440. Metabolic Engineering Communications 2016, 3, 24–29. https://doi.org/10.1016/j.meteno.2016.01.005.
(98) Tombari, E.; Johari, G. P. Structural Fluctuations and Orientational Glass of Levoglucosan—High Stability against Ordering and Absence of Structural Glass. The Journal of Chemical Physics 2015, 142 (10), 104501. https://doi.org/10.1063/1.4913759.

"Freeze crystallization is an industrial method use to remove water in form of ice from industrial streams. This method is efficient, robust and needs less energy to be operated than many other available methods. Freezing water from various streams can enable the production of novel sustainable textiles, renewable fuels and biodegradable products."

Aalto-DT 138/2023

ISBN 978-952-64-1412-6 (printed)
ISBN 978-952-64-1413-3 (pdf)
ISSN 1799-4934 (printed)
ISSN 1799-4942 (pdf)

Aalto University
School of Chemical Engineering
Department of Chemical and Metallurgical Engineering
www.aalto.fi

BUSINESS + ECONOMY

ART + DESIGN + ARCHITECTURE

SCIENCE + TECHNOLOGY

CROSSOVER

DOCTORAL THESES